Landform evolution in the southern central Andes: The major mechanisms of formation of the Santa Isabel escarpment, 34° to 38°S, Argentina.

By

Helen Neilson

Submitted in partial fulfillment of the requirements
for the degree of Honours Bachelor of Science in Earth Sciences.

At

Dalhousie University
Halifax, Nova Scotia

DALHOUSIE UNIVERSITY
UNIVERSITY
Inspiring Minds

Department of Earth Sciences
Halifax, Nova Scotia
Canada B3H 4J1
(902) 494-2358
FAX (902) 494-6889

DATE: April 27th 2007

AUTHOR: Helen J. Neilson

TITLE: Landform evolution in the southern central Andes: The major mechanisms of formation of the Santa Isabel escarpment, 34° to 38°S, Argentina.

Degree: B.Sc   Convocation: May 2007   Year: 07

Permission is herewith granted to Dalhousie University to circulate and to have copied for non-commercial purposes, at its discretion, the above title upon the request of individuals or institutions.

_____
Signature of Author

TABLE OF CONTENTS

LIST OF FIGURES

Abstract

In order to ascertain the mechanisms of formation of a 20 to 150 m high, 300 km long, N-S trending escarpment located between 34° and 38° S, Argentina, geomorphometric analysis of parameters such as sinuosity, topography, and local fluvial evolution were used to study regional features produced through fluvial and tectonic evolution. Surficial units were mapped based on the interpretation of 3 arc second DEMs and available geologic maps in order to place the escarpment evolution into regional context. The sinuosity of the escarpment face was found to range from 1.1 to 1.3 in the northern section, between 1.5 to 1.7 in the central section, and from 1.3 to 1.5 in the southern section, indicating that incision of the scarp has been greatest in the central region. Analysis of fluvial knickpoints on streams flowing east over the escarpment reveal a greater number and farther migration of knickpoints in the south than the north. The Rio Salado, which flows within 15 km along much of the escarpment, shows a significant knickzone situated near the central region. These and other geomorphometric analyses, mapped location of faults, and the interpretation of the regional topography suggests that this escarpment was formed though the parallel incision of the Rio Salado. The location and rate of Rio Salado incision is controlled by normal faulting and base level change. The local extension and consequent incision has also affected sedimentation patterns and incision history of major Andean streams that are tributaries of the Rio Salado.

Acknowledgements

Chapter 1.0 Introduction

The region between 32° and 38° South, Argentina, lies within a dynamic Andean transition zone between regions of flat slab and steep slab subduction (McIntosh,2004; Baker.,2005). In the middle of this transition zone, along the 67th longitude line, lies a N-S trending escarpment with an average central rise of 150 m. This landform, hereafter referred to as the Santa Isabel escarpment (after the nearby city), extends over 300 km in length. This is comparable to the entire 500km Niagara escarpment which partially encircles the great lakes. The escarpments general curvature runs similar to the Argentine coast line to the east, and its topographic cross section varies greatly from a 1-2m rise in its northern extent to 170m in its central point. This region is dominated by Plio-Pleistocene volcanism and backarc extension, and is situated at the convergence point of four major Andean Rivers. Though it is clearly surrounded by many possible mechanisms of formation, the origin of this landform remains undetermined.
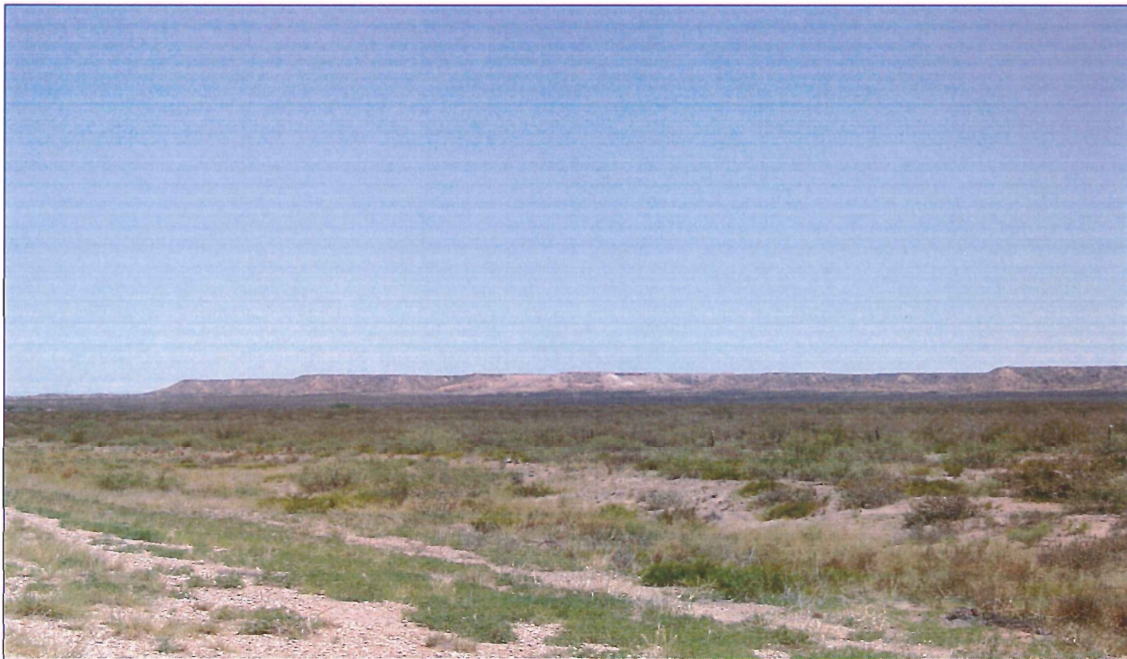
Figure 1.1 A distant view of the Santa Isabel escarpment. (Field, 2007, J.Gosse)
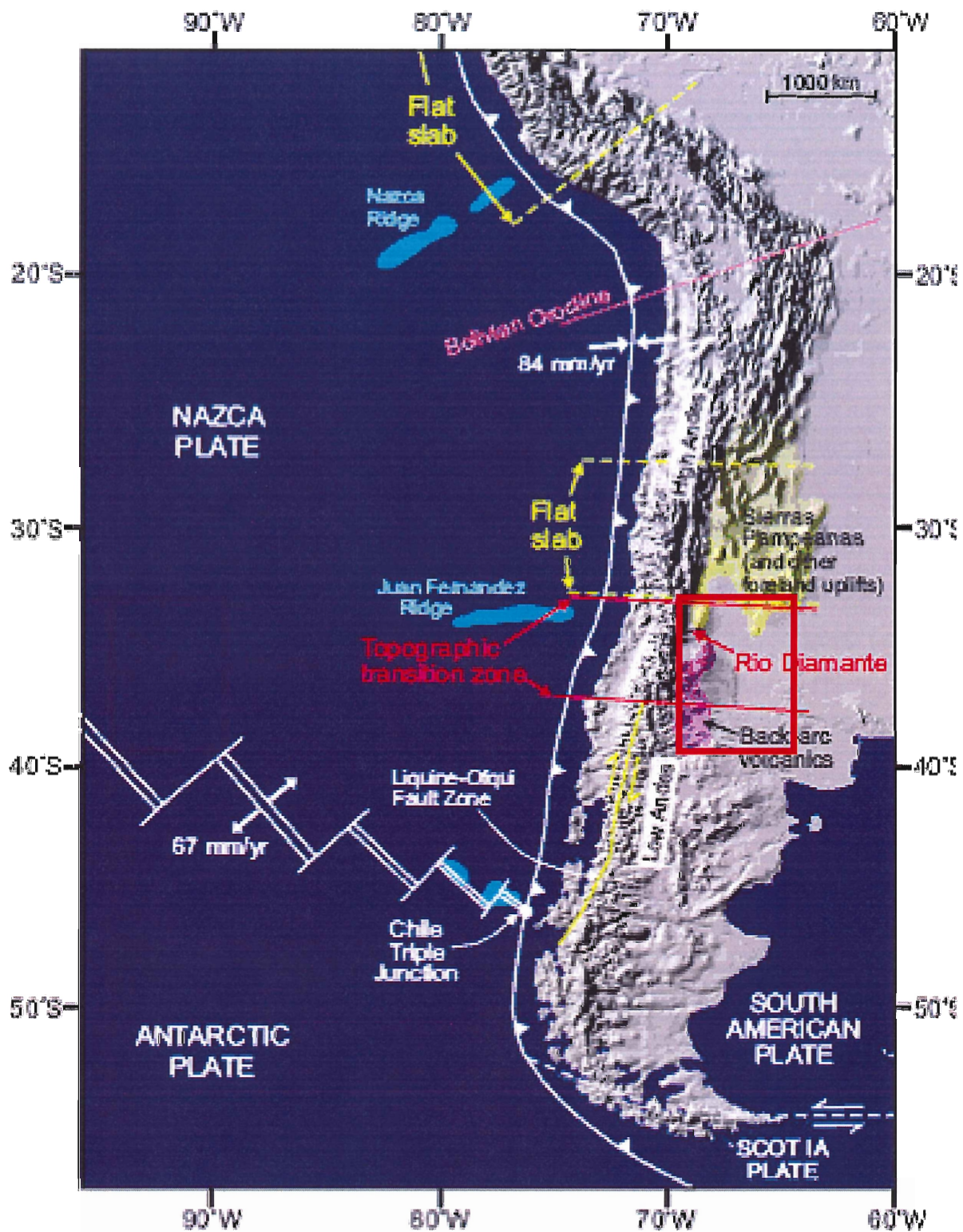
Figure 1.2 The large context of the study area: The region of focus is boxed in red, and clearly surrounded by varying tectonic conditions such as the flat slab zone and major uplift to the north.
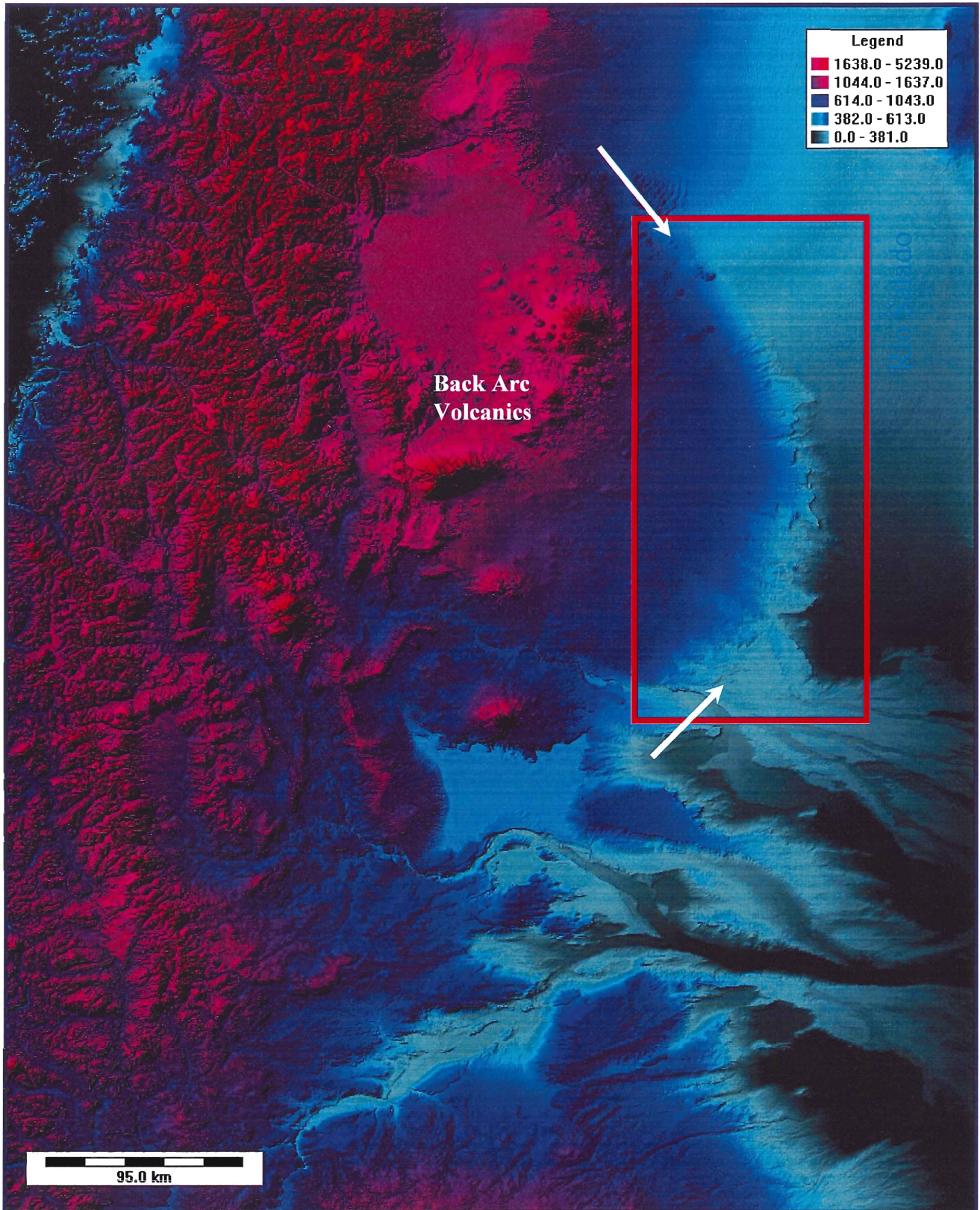
Figure 1.3 A DEM of the central study area, with a red-blue color scale to highlight the Santa Isabel escarpment, shown boxed in red.(Location 34-38° S). Legend is elevation in meters.

Four possible mechanisms of formation of the escarpment are: 1) the escarpment is a result of parallel incision by the Rio Salado; 2) the scarp is associated with concordant knickpoints propagated from the coast during lowstand periods in the Quaternary, 3) the escarpment represents a fault scarp, or fault line scarp formed as a result of recent leading edge thrusting related to regional shortening (eastward expansion of the Frontal Cordillera or San Rafael Block), or 4) the Santa Isabel escarpment is the west wall of a graben or series of grabens formed as a result of back arc extension.

The principal objective of this thesis is to test which of these mechanisms may have formed the escarpment using available and remotely sensed data. An additional objective is to assign a relative age of formation to the escarpment in relation to other significant events in the area. This includes the formation of the ubiquitous volcanic cones associated with fissures and possible back arc extension, and the deep incision of the pediments on the Andes eastern flank over the past 1 Ma, as documented by Baker et al, (2005).

Orogen-scale landscape evolution in the transition zone (McIntosh, 2004) is a reflection of crustal and mantle dynamics that are migrating southward in a wave as the obliquely oriented Juan Fernadez ridge is consumed by the South American plate (see figure 1.2), and of surface processes that are controlled by glacial-cycle climate variation and an associated latitudinal shift of climate patterns. To establish the rates and styles of tectonic and surficial processes that govern large scale (up to 10^5 km^2) post-Miocene landscape evolution, it is necessary to investigate key changes in the landscape over timescales of 10^5 to 10^7 years.

Chapter 2.0 Background

2.1 Location of the study area

The study area for this project includes not only the region immediately surrounding the escarpment (between 34.5° and 37.5ºS), but instead, most DEMs used to examine the landscape encompass the area between 32° and 38° S. This extended picture allows the mapping of various geomorphic surfaces, and thus permits inferences to be made pertaining to the influential mechanisms in the area, be they fluvial, volcanic, or tectonic.

2.2. Regional Tectonic Setting

Significant physiographic changes occur in the Andes at 35° S. The width of the mountain belt itself is thinned south of this latitude, and there is a gentle decrease in mean peak elevation from 5000 to 3000m, which is accompanied by an abrupt decrease in relief (Kennan, 2000; McIntosh, 2004). This topographic change is believed to be the result of an alteration in the angle of the subducting slab (e.g Jordan et al., 1983; Yanez et al., 2001). Through analysis of the spatial distribution of major seismic events, it is suggested that the slab dips very shallowly, at about 10°, in the flat slab zone to the north (Allmendinger et al., 1983; Montgomery et al., 2001). This dip has caused the continuous spread of compressive deformation in the foreland direction during the Pliocene and Quaternary. The dip of the subducting slab is much greater to the south (about 30°). In the foreland basin large units of basalt indicate recent extension (Jordan et al, 1983). The geology of the transition area indicates the change in angle of the subducting slab in that the principal volcanic fields are found only to the northern extent of about 34.5° (see fig 1.2). Smaller scale uplifts occur in the southern area of the transition zone. Other causes

of the changes in topography in this zone include that the amount of shortening across the range decreases from north to south. (Introcaso et al., 1992; Ramos et al, 1996.) Because the type and magnitude of a deformational event occurring in a given region depends on the structure and rheology of the crust, the area must also be examined in the context of past events and processes which may affect these parameters. Such events in the Andes vary with latitude, and have taken place as far back as the Paleozoic. Latitudinal climate variations can also play a role in geomorphologic evolution, for example, influences such as precipitation trends can change erosion rates. At about 33° there is an increase in the mean annual precipitation received on the eastern side of the range (Montgomery et al.,2001). The lowering of mean elevation level and decrease in relief between 34°and 37° may also be partially attributed to the presence of the perennial snow line crossing the area. Higher erosion rates also result from the presence of permanent glaciers in the southern region.

2.3 Geologic History

The Principal Cordillera, in the transition zone, was subjected to its most recent cycle of strong tectonic activity between 10 and 14 Ma (Baldauf,1997). During this time the thrust front moved further east and meeting a large fault, which initiated the formation of a small plateau trending N-S. A second period of magmatism then occurred, resulting in explosive andesitic volcanism (Baldauf, 1997). The arc magmatism that is currently present along the continental divide was established in its position by the mid-Pliocene. Folding and thrusting had also ceased by this point (Giambiagi, 2003b).

During the Quaternary, a significant amount of the folding and thrusting took place creating the Precordillera (Jordan et al, 1983, Giambiagi et al, 2002). The areas to

the South of this region have also experienced continued structural inversion and uplift (Jordan et al., 1983). The Rio Tunuyan and other rivers have undergone flow path changes as a result of this uplift; where the system and its tributaries used to flow to the east across the piedmont, it now flows north, and is diverted around the new uplifted highlands (Polanski, 1963). The tectonic environment from 33° and southward involves the primary direction of compressive stress in the main cordillera and the fore-arc shifting from E-W in the Pliocene, to NNE-SSW in the Quaternary (Lavenu et al., 1999). North of 34.5°, however, there are fewer known accounts of E-W compression since the Quaternary. The fact that there are large amounts of back arc basalts deposited in the area to the east of the Principal Cordillera implies that the primary tectonic mechanism in the area is likely crustal extension and thinning (Jordan et al, 1983). The presence of basaltic volcanism in this area supports the idea of an extensional regime.

In the areas to the North of Rio Diamante there are some shorter fracture zones which have a E-W orientation. This trend is followed by several Quaternary volcanic centers to the south.

2.4 Application of knickpoint migration to landscape evolution studies

Knickpoints in a river system are formed when there is some type of base level change, be it to due to sea level fluctuation, tectonically driven, or the result of other factors. After experiencing this change in channel path, the river system will attempt to restore slope equilibrium through headward erosion. This shows up in a channel profile in the form of a knickpoint, or a notable change in gradient over a short distance.(Ritter et al, 1995). More erosive knickpoints which have a change in gradient over a larger distance are termed knickzones. Headward knickpoint migration is highly dependant on

7

both the structural and stratigraphic nature of the host rock, which makes it very important to take into account the regions geomorphologic history and current geologic conditions. In channels cut through material lacking cohesion, for example, the knickpoints which result will be smooth with only a short amount of upstream migration (Ritter et al, 1995). If, however, a channel cuts through cohesive sediments, or bedrock, the knickpoint could retreat for a much longer distance while maintaining a vertical headcut.

In 1987 Gardner proposed that there are three basic models by which knickpoint evolution can occur. These are dependant on the shear stress produced in the river flow, balanced by the shear resistance of the parent material. When a knickpoint face is inclined, there is a uniform change in its slope, and the angle is dependant on the resistance of the channel material. This measure of resistance determines if the river strength is enough to move the sediment from the front of the knickpoint. In instances where the sheer stress needed to entrain the sediment is less than the strength of shear stress the river holds, aggradation of the material occurs, and the gradient is adjusted. The second model is called parallel retreat, and it recognized by the headward movement of a near-vertical knickpoint face which has small to no changes in slope inclination. Parallel retreat occurs in its most recognizable form when layering is present in the host material in a manner that has a more resilient material overlies a less resistant layer. Knickpoint replacement, the third model, takes place when erosion occurs upstream from the knickpoint as well as on the face itself. This produces a profile that shows two zones which have been modified from their original shape.

Knickpoint patterns provide a directional basis with which to compare each of the possible mechanisms of scarp formation. This data, combined with relevant mapped information such as the major geomorphic surfaces, the presence and directional movement of regional faults, and the climatic and precipitation trends over time, serves to help determine the likely mechanisms of escarpment formation.

Chapter 3.0 Methods

Because most of the analysis of the study area was conducted remotely using digital elevation models, GIS programs such as Rivertools®, and Arc Map®, were invaluable in regional examination, and in representation of relevant geomorphic variables. All DEMs where downloaded from data provided by the U.S. Geological Survey, EROS Data Center, Sioux Falls, SD, on seamless.usgs.gov. Gaps in data on the 3 arc second SRTM DEMs where infrequent, and are mentioned when they may cause distortion in data interpretation by a program.

3.1 Mapping of surfical geomorphic units

Geomporphic surfaces such as alluvial fans and pediments were mapped on a 3 arc second DEM according to structure and topography, and based on compiled geologic information and research. Because much of the extent of these units is based on visual interpretation of landforms in a DEM, the map produced cannot be taken to infer anything below the surface deposits.

3.2 Mapping of faults

In order to examine the hypothesis that the escarpment may be either a fault line scarp, or related to faulting events associated with the eastern grabens, faults and inferred faults from the geos map of the La Pampa Provence, and the Medoza province, were mapped over the existing river systems to determine if there was a relationship, and individual faulting events were examined in terms of displaced material.

3.3 Escarpment Parameters

3.3.1 Topographic profiles of surfaces

The basic characterization and geomorphometry of the Santa Isabelle escarpment was derived from both Digital Elevation Models and from geologic maps. Topographic profiles of the length and width of the landform were found using line profiles in Rivertools®. Comparisons were made in topographic profiles between the escarpments elevation patterns and those of the surrounding landforms. Where the vertical exaggeration of the display was less than 5, the slope of given landforms could be calculated and potentially correlated with other formations, when taking into account changes in deposition.

3.3.2 Sinuosity of the escarpment

A possible method of analyzing the amount and type of erosion along the face of the escarpment is to measure the average sinuosity for a given length, and compare these readings as they progress along the extent of the face. A highly sinuous face accompanied with a steep slope is indicative of large amounts of fluvial erosion, while a gradual sloping straight face represents less eroded material. Extremely straight measurements with a sharp, steep slope would suggest proximal faulting.

The sinuosity of the edge of the escarpment was found using the formula L1/L2, where L1 is the true length, or distance covered by the escarpment, and L2 is the straight length. In order to represent the general trend of sinuosity, the lengths were first measured in increments of 10km (straight length). In attempting to increase precision, the measurements were made again using increments of 5 km and the sinuosity was again plotted.

3.3.3 Scarp Degradation

In an attempt to estimate differences in the degree of erosion along the fan-pediment complex and the escarpment face, the principles of diffusion were applied to data provided by a representative slope taken from a high resolution Rivertools DEM. Diffusion modeling was used to provide an estimate for the transport of sediment and evolution of a hill slope as erosion occurs. In this case, the presence of the $CaCO_3$ cap means that these readings will not be entirely accurate as the cap provides a significant reduction in the rate of erosion on the upper region of the escarpment, but a general trend may still be represented. To quantitatively estimate sediment diffusion, the continuity equation states $\delta z/\delta t = \delta R/\delta x$, where z is the elevation at a given point on the slope, x is the horizontal distance, t is time, and R is the rate of sediment flux. To calculate the rate of sediment transport one must integrate a diffusivity constant (k), and the gradient of the given slope. For the environment given, the diffusivity constant used was $k = 1m^2/ka$. This is based on the average k used by Hsu and Pelletier., 2004, for their work on alluvial fans in the semi arid southwestern US. Work by Nash, 1974, also provided a valuable base on which to form ideas about scarp evolution and morphology.

3.4 Long profiles of streams and knickpoint recognition

As previously stated, knickpoints and knickzones are caused when a fluvial system experiences a change in gradient caused by base level lowering, which initiates or enhances headward erosion of the system, causing a knickpoint. As the river channel works to restore equilibrium, the knickzone propagates backward, and is often smoothed out.

Previous work on landform evolution related to the investigation of fluvial knickpoint formation by Zaprowski et al., (2001), and regional work by Baker, (2005) prompted the mapping of the local paleo-drainage system in order to search for knickpoints. To analyze these problems, the drainage network (including current and paleo-channels) was firstly defined using Rivertools. Six representative channels (shown in figure 4.4.1) running across the escarpment were selected by initially mapping the river network on a multilayer plot, and then ordering each stream according to their Strather order (a measure of magnitude between small tributaries and large rivers). Streams below order 6 were pruned, as they would have a relatively small erosive force. Finally, a range of regional channel profiles which seemed to indicate potential knickpoints were selected. After examining individual long profiles of each paleo channel, these were normalized for the distance from the escarpment, and plotted together. Knickpoint numbers and distances from the escarpment were then plotted on each channel and compared with the other channels in order to determine if there is a pattern between propagation or number of points. This pattern could potentially indicate from which direction the erosional force originated and moved, and with what strength it influenced the individual river channels. Whether the distance between concurrent knickpoints varies significantly in different streams, or is equidistant, also suggests whether the escarpment was formed through fluvial incision or through faulting, respectively (Figures 3.1 and 3.2). To confirm the observed trends, six further channels were selected and examined along their entire channel profiles for knickpoints. Finally, a channel profile of the Rio Salado (running parallel to the escarpment) was also taken to

analyze for the presence of knickpoints or zones, and to test whether there is a correlation between this major system and the smaller channels on the escarpment.
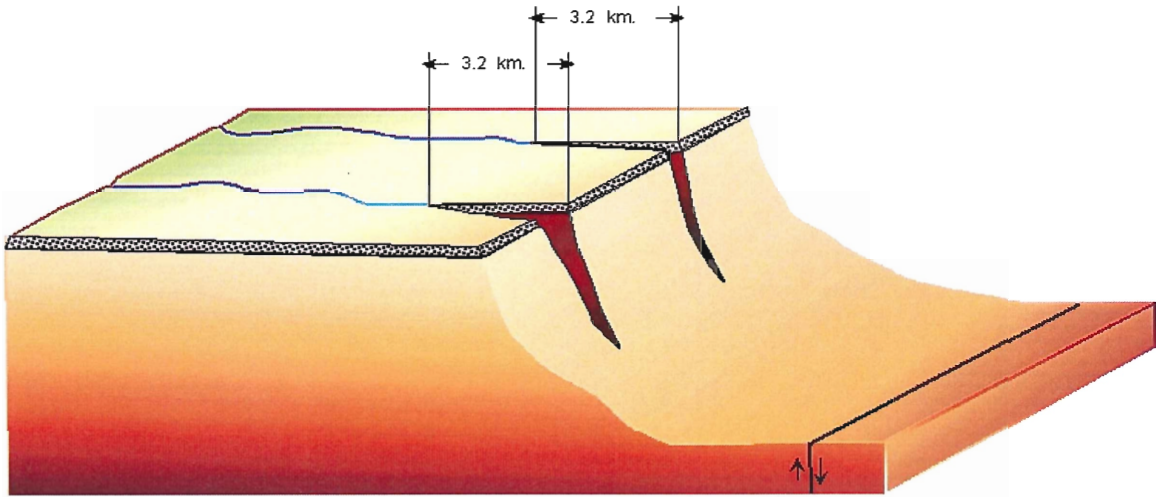
Figure 3.1 Parallel knickpoint migration controlled by faulting.
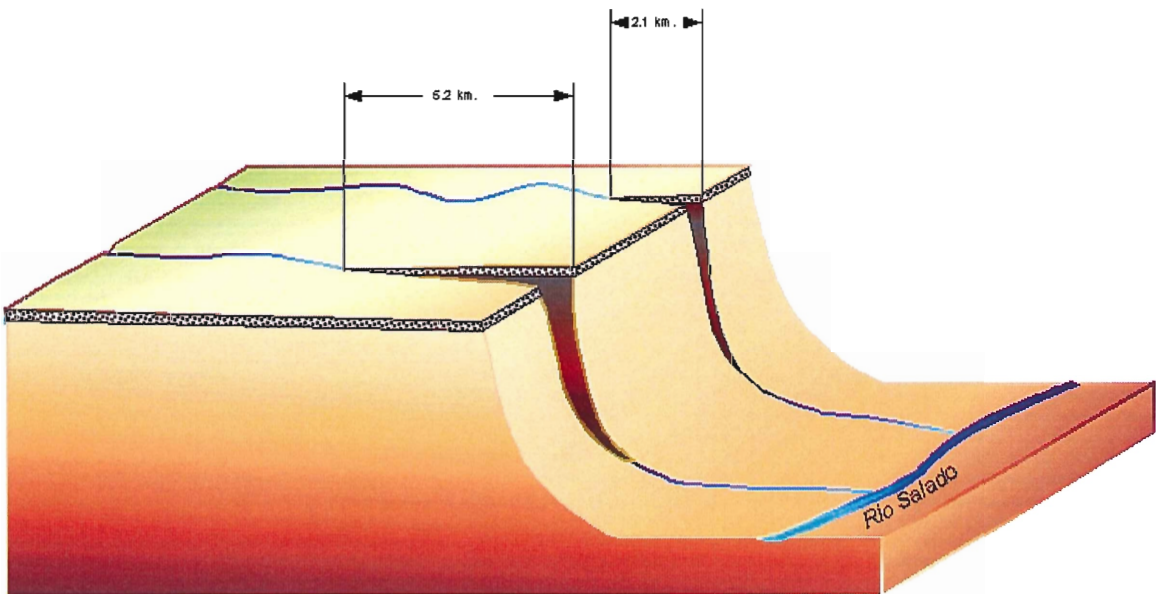
Figure 3.2 Uneven propagation of knickpoints due to incision from the Rio Salado.
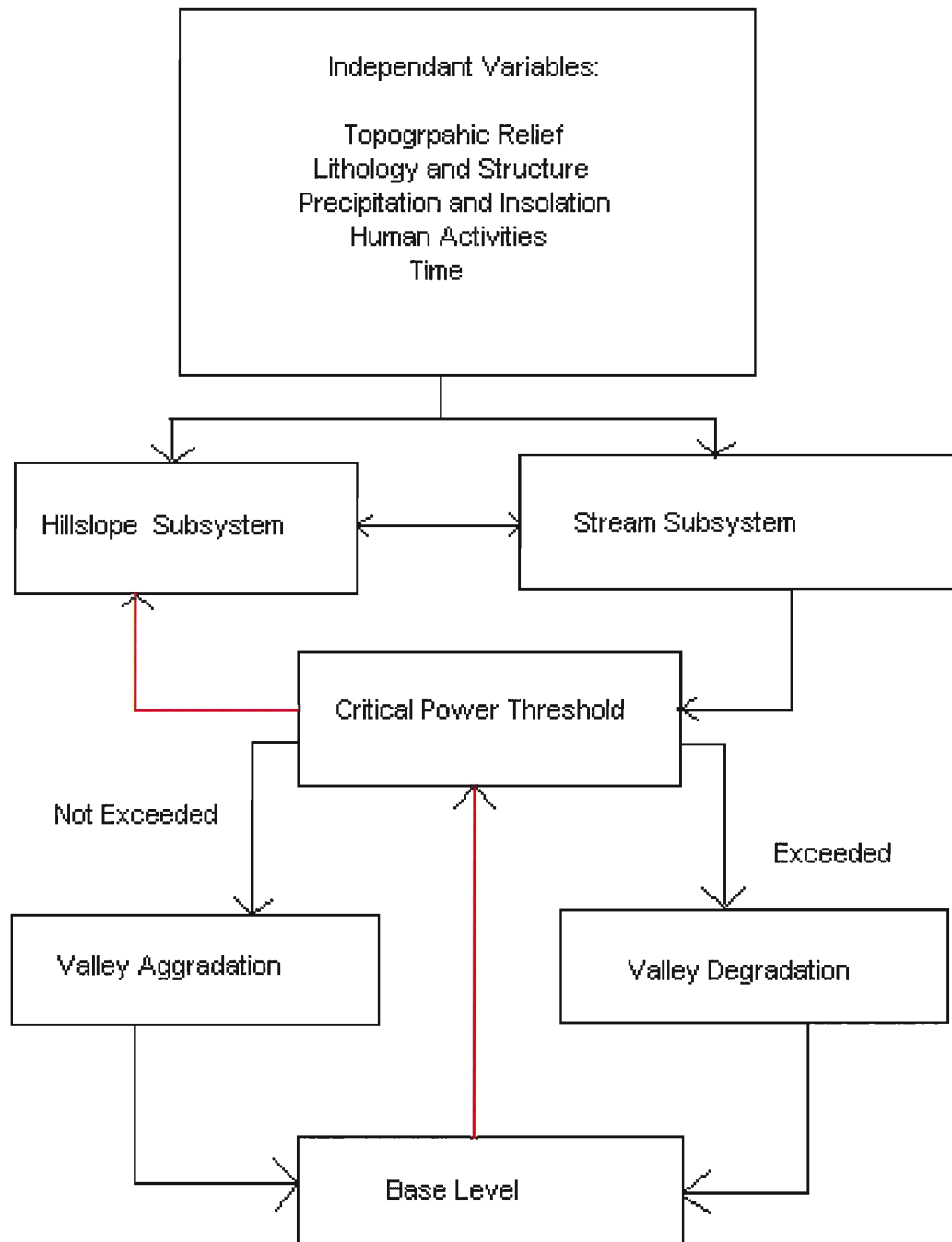
Figure 3.2.3 Fluvial influence flow chart.(from Bull, 1991)

Finally, this flow chart shows the various parameters which must be taken into account when examining a stream system in general. It also demonstrates the paths which can lead to base level change due to erosion. Key points include the fact that base level is

directly linked to the critical power threshold, which means that a change in base level initiates an increase in stream power, and thus an increase of erosion, which is the basic principal behind knickpoint formation. It is also important to note that these variables are all interconnected and controlled by variables such as precipitation, topography, and human activity, which must be factored in when conducting any stream system analyisis.

3.5 Evolution of the carbonate cap

Under examination in the field the Santa Isabel escarpment was found to be overlain by a 3m thick $CaCO_3$ cap. The mapped extent of the carbonate was later available from geologic data, and has been reproduced as observed in the results section, and as inferred in the interpretation. The sample taken of the interpreted pedogenic carbonate cap (collected by Dr.Gosse, 2007) was briefly examined in thin section in an attempt to determine whether it is indeed pedogenic, or could possibly be classed as vadose or another form or precipitated $CaCO_3$. Although this is not directly related to the evolution of the Santa Isabel escarpment, it is undeniable that the cap plays an important role in its preservation. The nature of the caps formation could also allow inferences to be made about the paleoclimate at the time of formation. This work is shown in the appendix, section A1.

A representative sample bearing finely laminated $CaCO_3$ has been sent to the Berkeley Geochronology Centre for U-series dating. When this age is available it will provide a constraint on the maximum age of escarpment.

Chapter 4.0 Results

4.1 Mapped Geomorphic Surfaces

Figure 4.1 shows the mapped geomorphic surfaces overlying a DEM produced in Rivertools. The influence of fluvial systems on the geomorphology of the area is immediately clear through the observations of the large, preserved alluvial fans seen in blue. Pediment surfaces and further alluvial deposits are also represented. When this is combined with the geology of the area it is interesting to note that the preserved surfaces show the presence of the same type of Pliocene carbonate cap which is believed to overly the escarpment to a greater extent than represented on the geologic map. It is likely that these alluvial surfaces are preserved greatly due to the presence of this cap in the same manner as the escarpment. Alluvial deposits of a similar nature are found in the fan surfaces in the south central fan, from the late Pliocene. The mapped volcanics are found to vary from Permian volcanic cones, to Miocene basalts and andesites, to Pliocene and Holocene basalts. Figure 4.4 is a representative surface zoom of one of the many volcanic cones in the region. This Miocene andesitic cone has a collapsed central region, with an active parasitic cone and several defined flows. Possible faulting events are mapped only according to perceived movement in the geomorphic surfaces in this case, to be later compared with the geologic maps, and possibly accepted as extrapolations of known events. Faulting is evident in the area even without the geologic data, as is seen in Figure 4.3, which shows a relief zoom of a graben caused by a significant faulting event on the escarpments northern flank. The second interpretation of the geomorphic surfaces, based also on field observations, helps to define the landform carrying the escarpment as a pediment- fan complex, and potentially extrapolate that it once continued to the east.
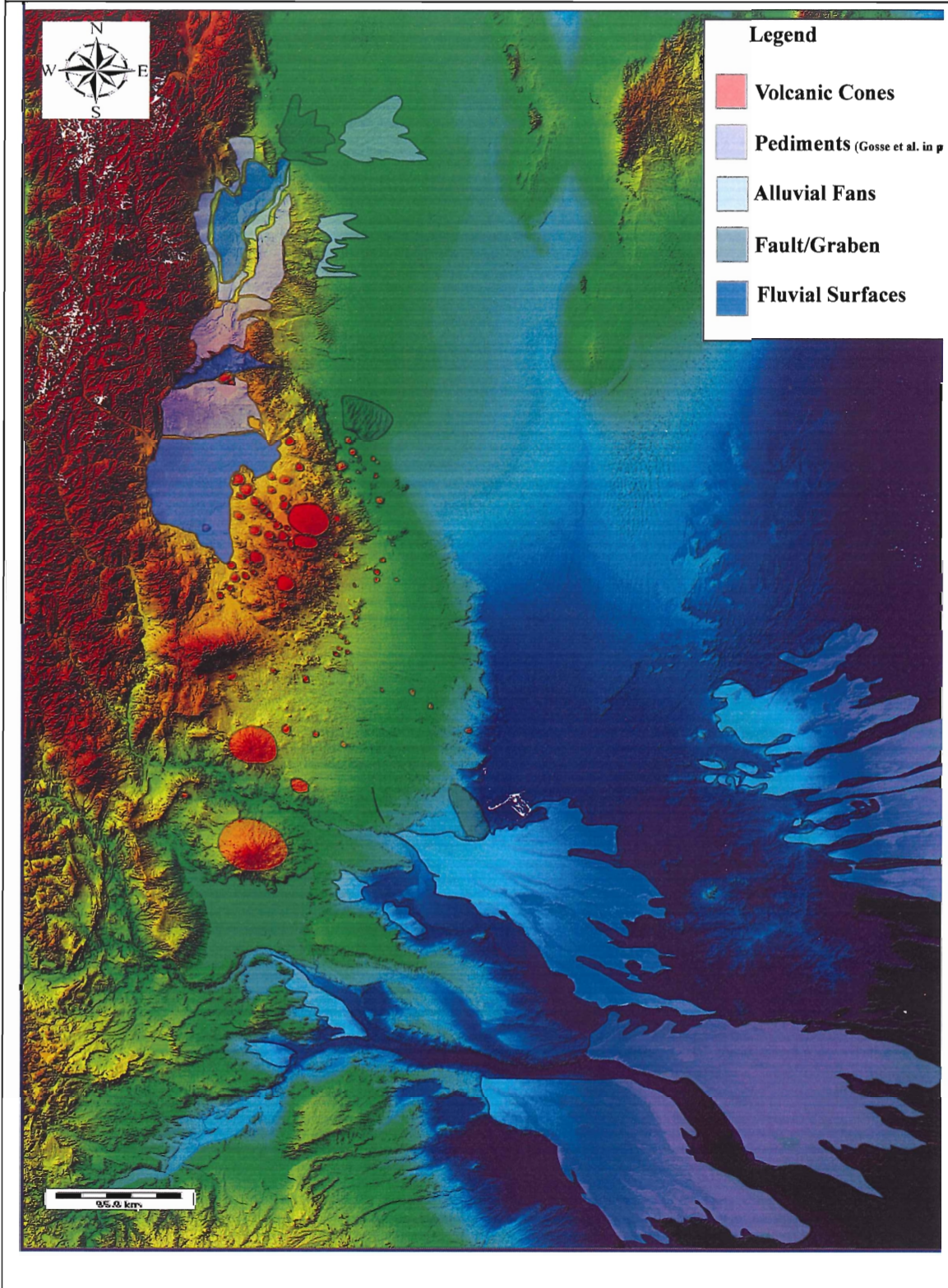
Figure 4.1 This map is the first interpretation of the surficial geomorphic surfaces in the study area. Note especially the large presence of defined alluvial fans and volcanics.
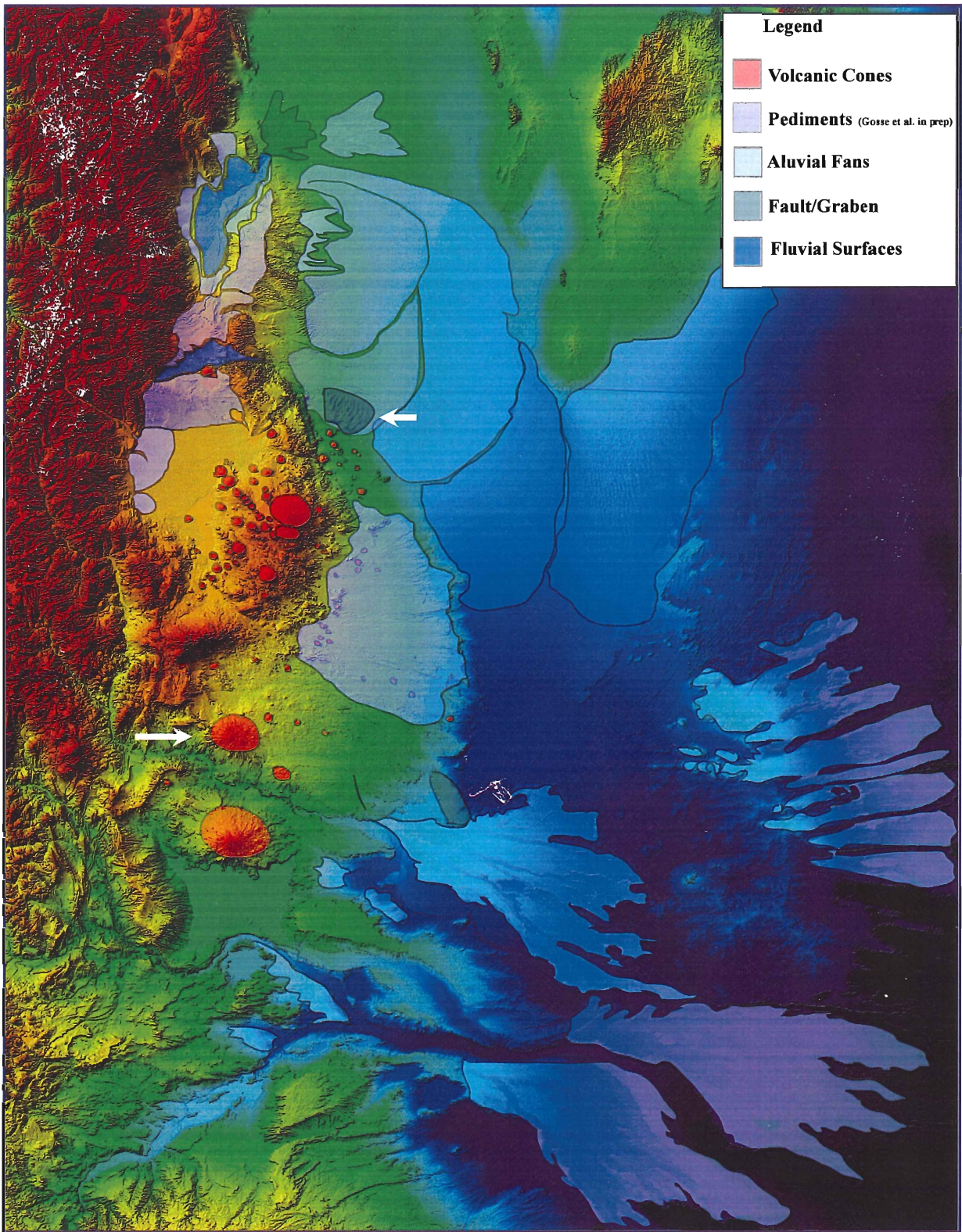
Figure 4.2 This is the second interpretation of geomorphic surfaces based partially on field observations by J. Gosse, and new observations on the DEM. White arrows show locations of relief zooms shown on page 20.
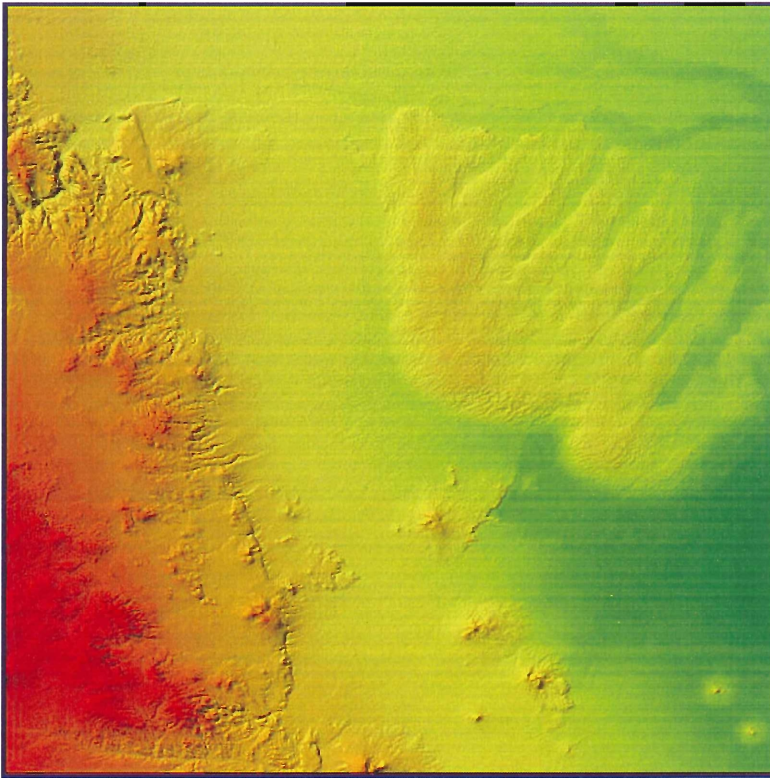
Figure 4.3 Relief zoom of the northern graben. 3 arc second DEM, (Rivertools).
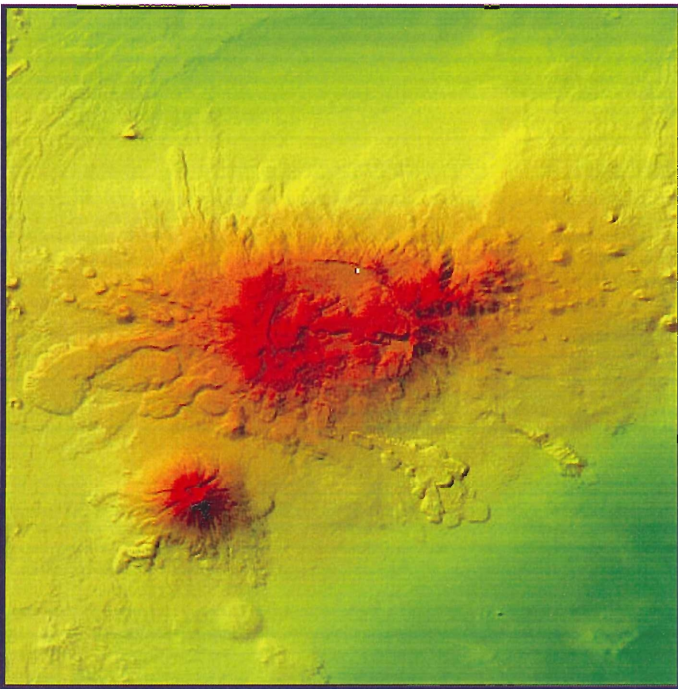
Figure 4.4 Relief zoom of an example collapsed volcanic and parasitic cone with visible flows. 3 arc second DEM (Rivertools).

4.5 Mapped faults and rivers
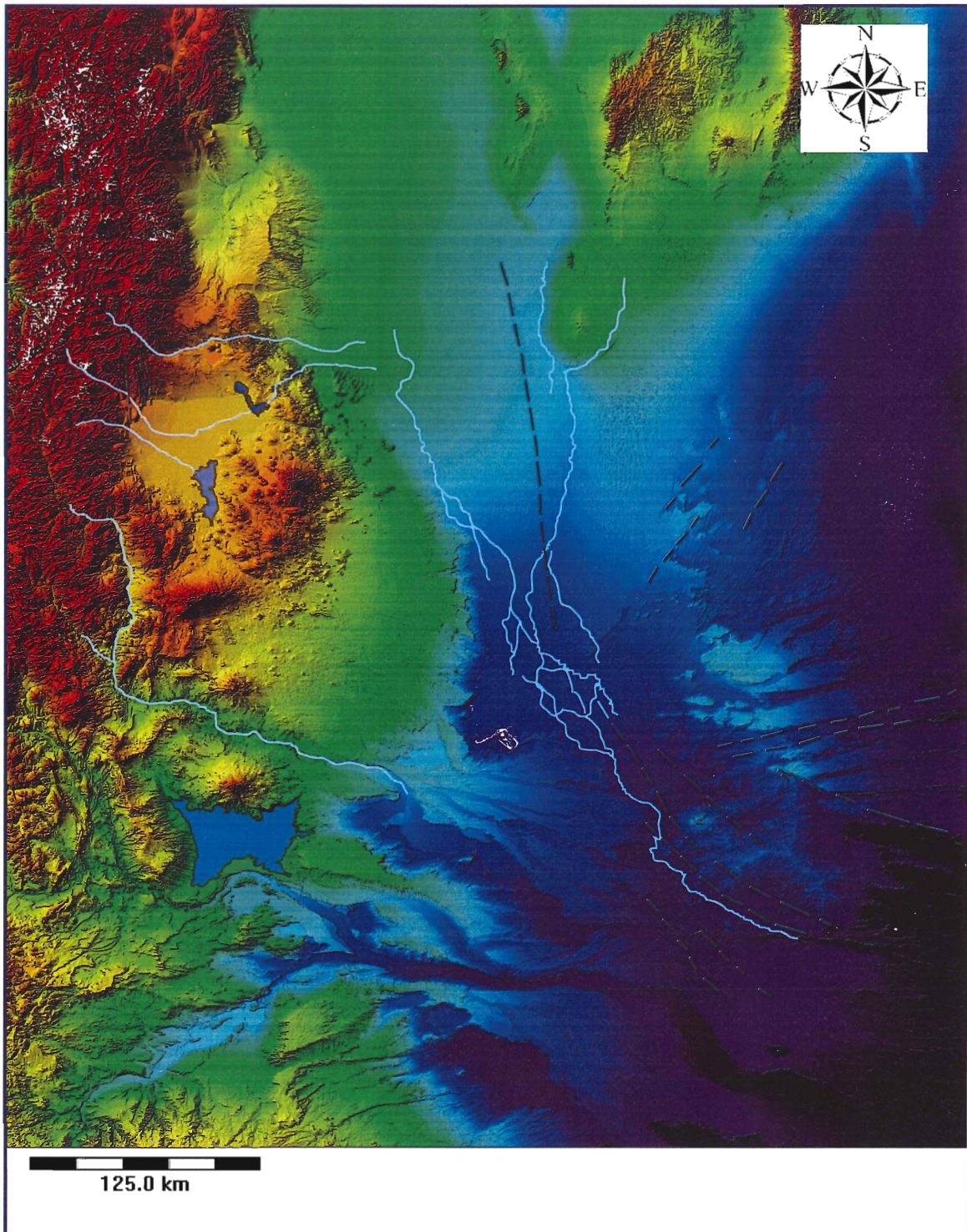
Figure 4.5 Rivers and Faults.(Rivertools) This image is meant to demonstrate the relationship between the major rivers of the area, and the large faulting events. River paths and fault traces from *Mappo geologico de la provincial de La Pampa* (Nielson., et al., 1999). Note the general trend of the rivers follows the direction of the faults.

The known and inferred faults from geologic data by both Nielson et al., 1999, and Nullo, 1993 were mapped on a DEM along with the main river paths in figure 4.5. This is meant to demonstrate the observed trend in which the major river systems in the area appear to follow the faulting events.

4.3 Details of the Escarpment

4.3.1 Topographic profiles of surfaces

The pediment-fan complex that the escarpment truncates has a significant convex profile as seen in Figure 4.6 (See figure 4.7 for profile location). Topographic profiles running E-W were taken in the northernmost region, an average central profile, and a profile from the southern region (Fig 4.3.3 to 4.3.5). These profiles reveal the differences in the smoothness and gradient of the fan-pediment complex, as well as representing changes in the scarp height from north to south.
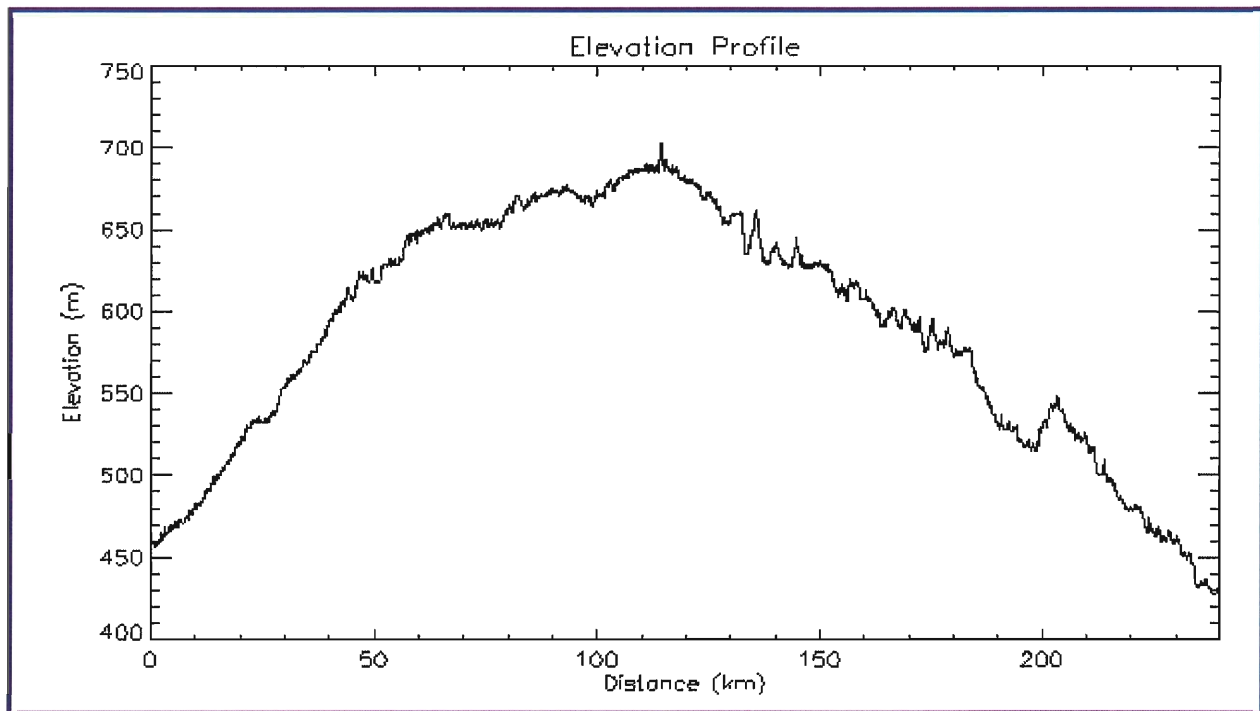
Figure 4.3.1. Line profile showing topographic variation in fan pediment complex height from N-S. Note extreme variation of over 100 m in elevation between northerly and southerly peaks.
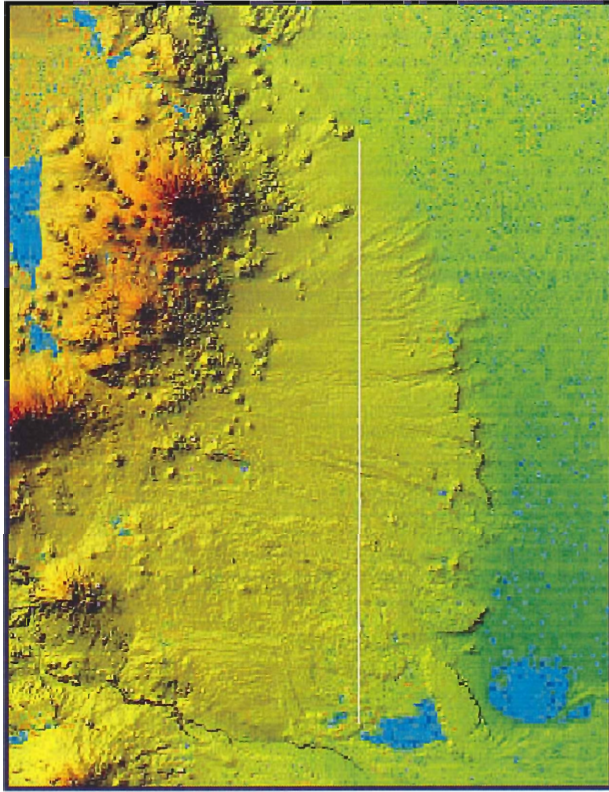
Figure 4.7 The white line marks the line profile taken in figure 4.3.1, which is meant to be representative of average topographic variation across the escarpment complex.

It is interesting to note that unlike the other profiles, the northern region does not contain a scarp at the change in slope. In comparison, the central profile (fig 4.9) has a steep undercut face. The southernmost profile (figure 4.10) has a somewhat anomalous slope partially attributed to the fact that it contains some areas overlain by basaltic flows, and others with newer alluvium. Note that the scale is varied on the following topographic profiles.
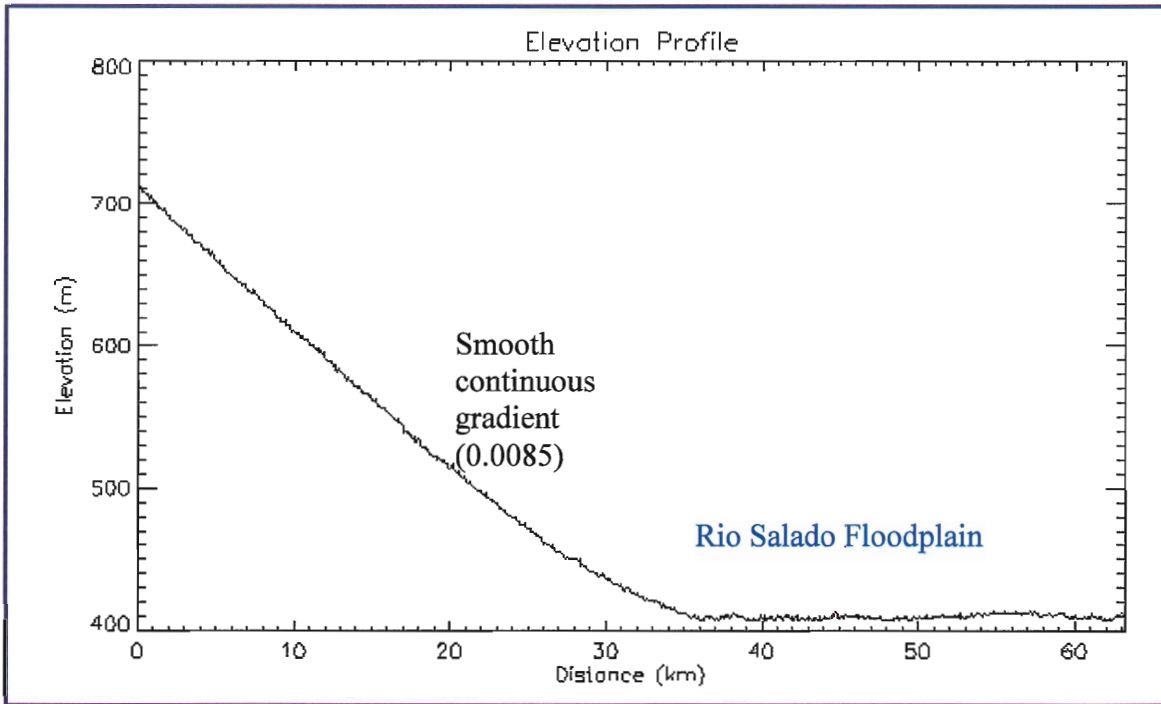
Figure 4.8 Elevation profile representative of the northern region of the escarpment.
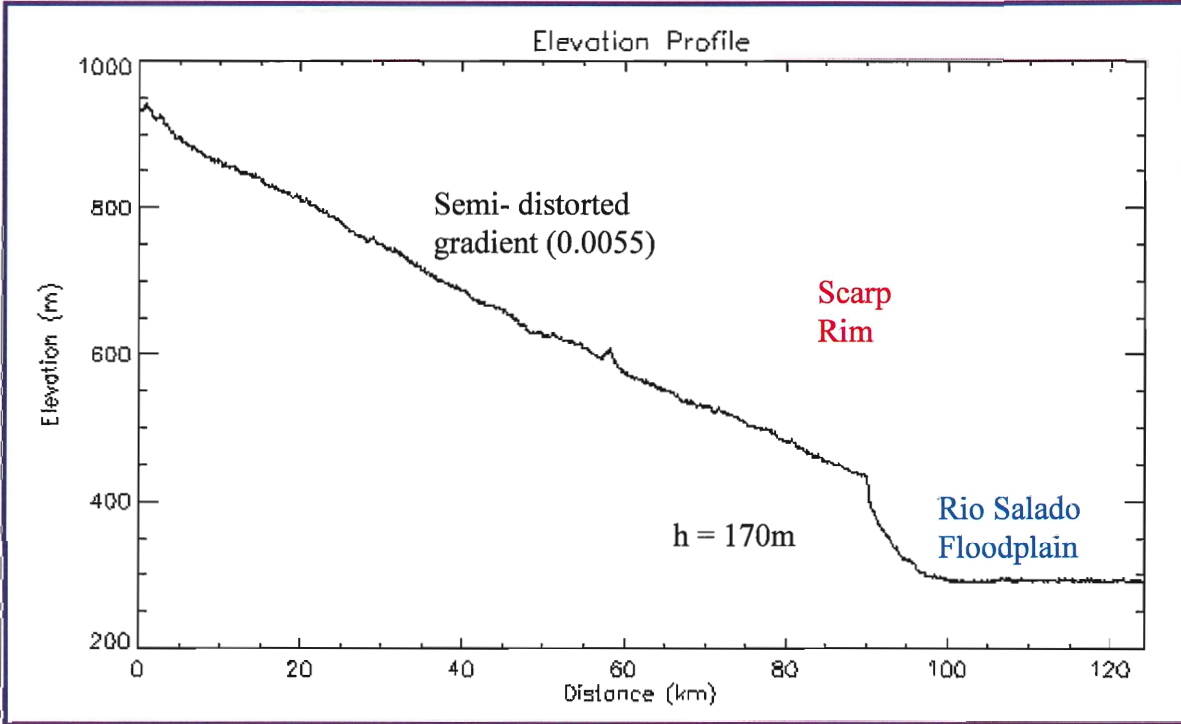
Figure 4.9 Elevation profile taken from the central region of the escarpment.

25
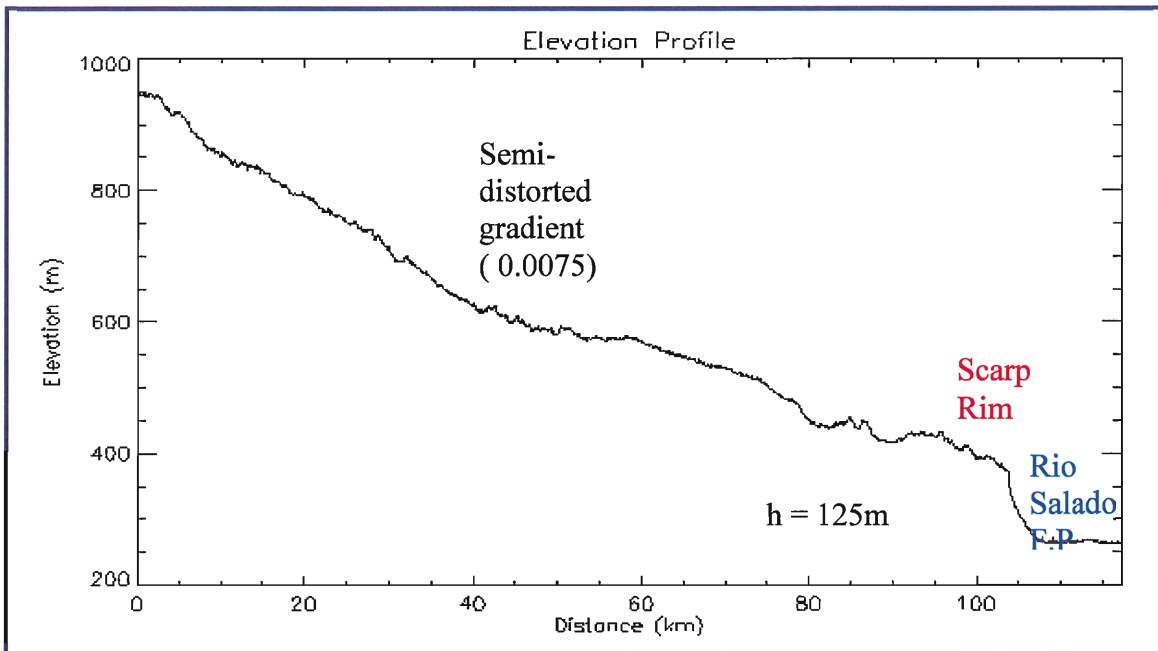
Figure 4.10 Elevation profile showing a representative slope from the southern region of the escarpment. Irregularities in this slope are partially due to minor basalt flows. (Elevation profiles: Rivertools.) (Nielson et al., 1999)

The differences in profile slopes along the NS range of the escarpment can also be compared to a general model for escarpment slope development over time. In figure 4.3.6 the north slope more closely matches the older more eroded profiles, while the central and southern slope retains a fresh face and slope, as per the younger deposits. While this may potentially be taken as evidence for the location of newest erosion, this does not take into account the presence of the cap rock, nor does it include the possibility of continuous fluvial erosion.
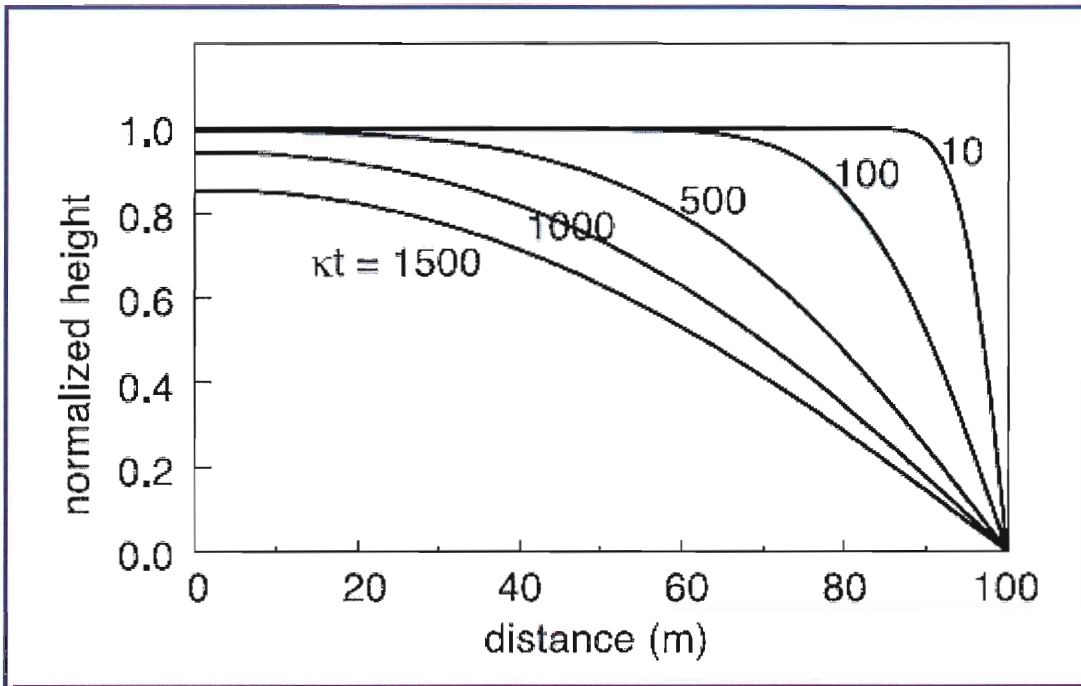
Figure 4.11 Representative elevation profiles of escarpment height and slope based on erosion over time. This figure does not take into account the cap rock of the Santa Isabelle escarpment, but serves to depict the general expected trend of erosion specifically on the scarp face.(Figure from Hsu and Pelletier, 2003.) Kt is the diffusivity constant, or rate of erosion based on a given material and its environment.

4.3.2 Sinuosity and Degradation

The resultant graph from the sinuosity measurements taken in 10km intervals, or windows, is shown in figure 4.3.2a. All measurements were made using line profiles in Rivertools. Figure 4.3.2b is the graphed trend using 5km intervals. It was found that the larger increment was a better representation of sinuosity as a trend. A straight line measures at 1.0 on the sinuosity scale, while anything above 1.5 is considered sinuous. The average sinuosity in the north was ranged between 1.1 and 1.3, central sinuosity measured between 1.5 and 1.74, while the sinuously in the south ranged from 1.3 to 1.45.

Sinuosity of the escarpment: 10 km intervals
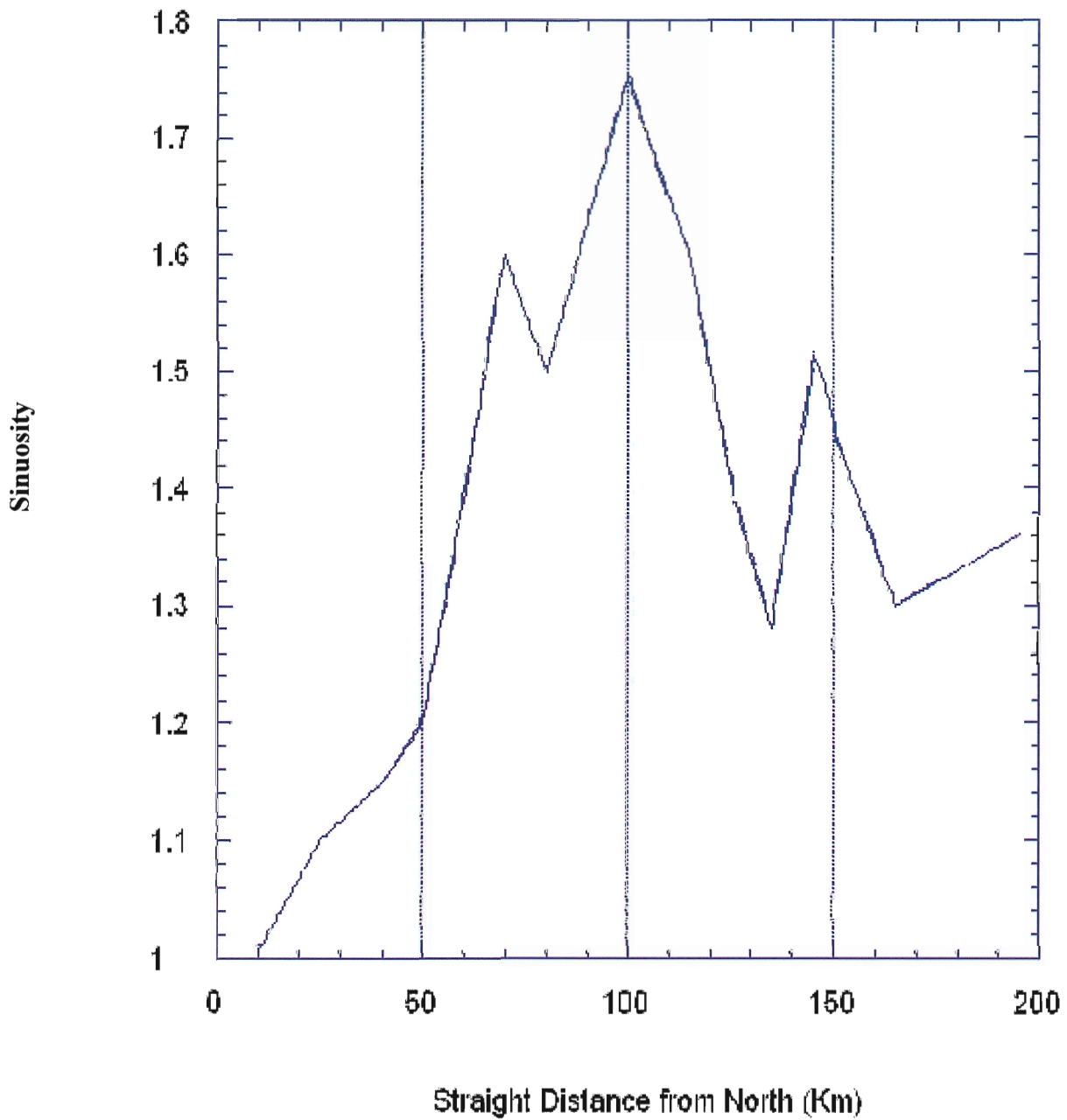
Figure 4.12 Sinuosity of the escarpment face measured over 10km intervals. This curve was accepted to represent the overall trend of sinuosity over the escarpment.

Sinuosity (5 km window)
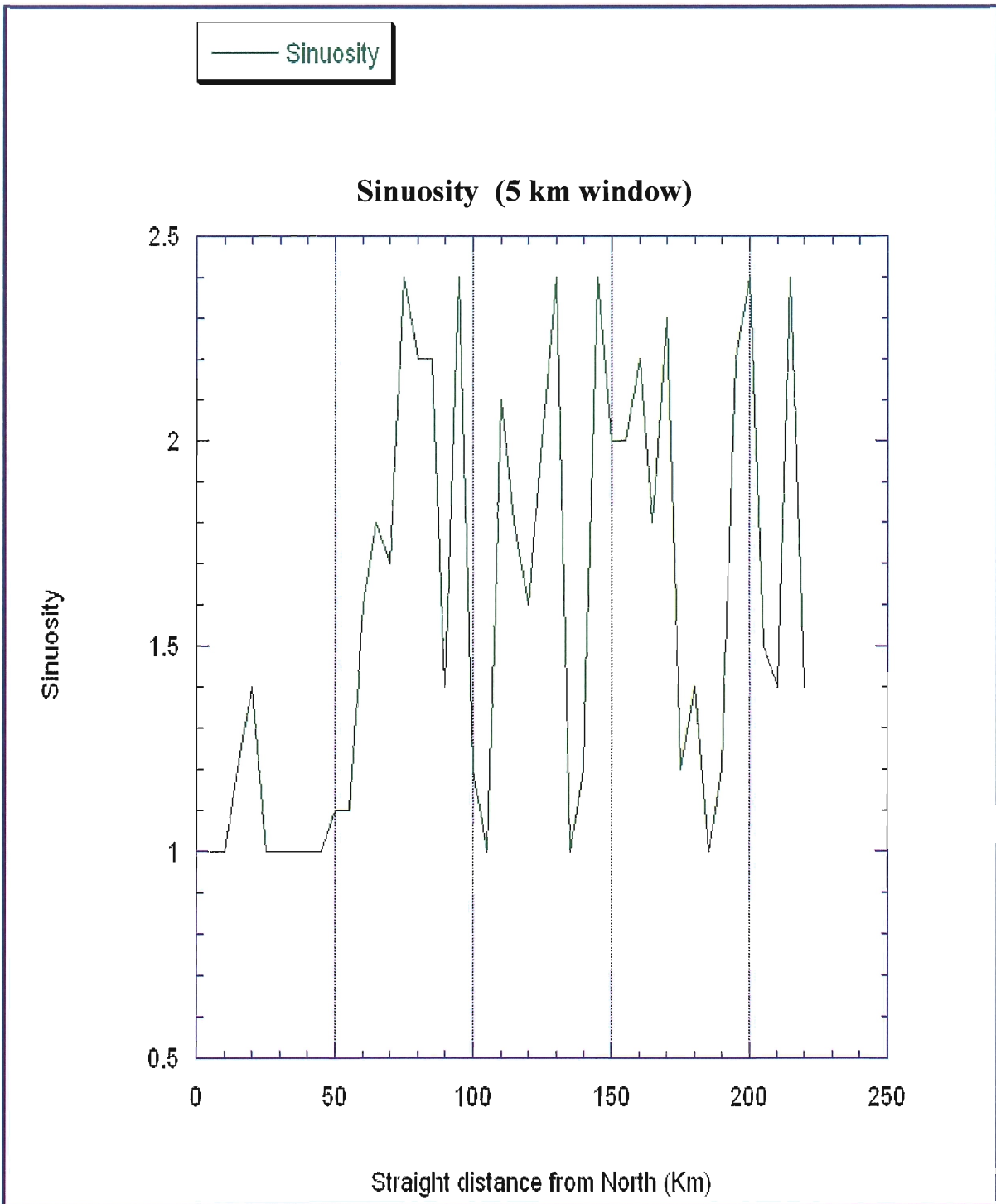
Figure 4.13 This figure was produced using the same methods as figure 4.3.2a), but using a 5 km window to improve precision. The resultant curve is less representative of the sinuosity trend over all.
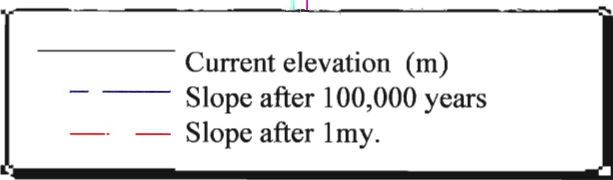
Figure 4.3.3 This graph is an estimate of erosion rates represented by change in elevation over time. The projection was found using diffusion modeling, based on selected slope points ($k = 1m^2/ 1ky$). This data does not take into account the presence of the carbonate cap, and is therefore only accepted as a general trend.

Legend:
— Current elevation (m)
– – Slope after 100,000 years
—·— Slope after 1my.

Erosion over time

Elevation (m) vs X Distance (km)
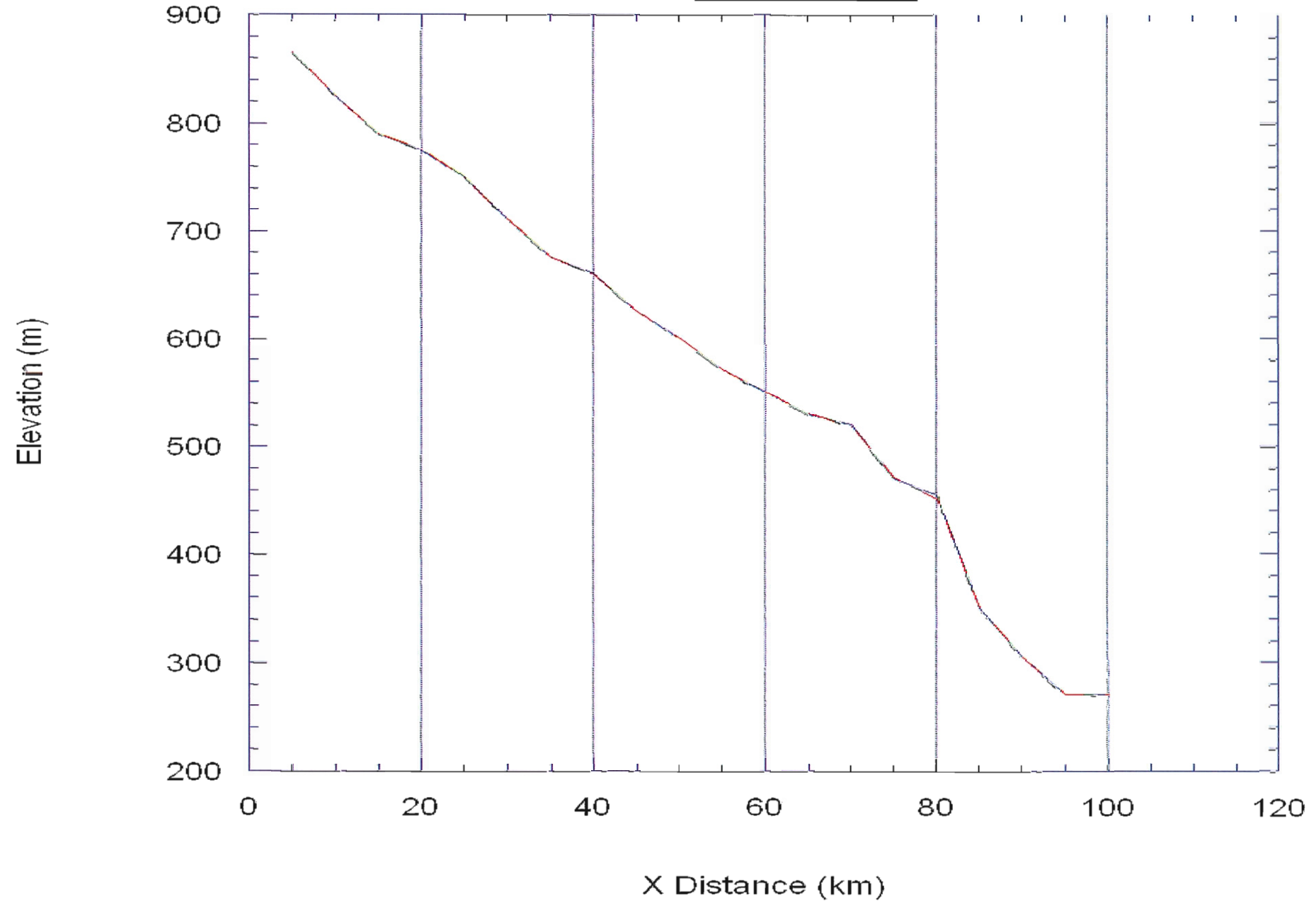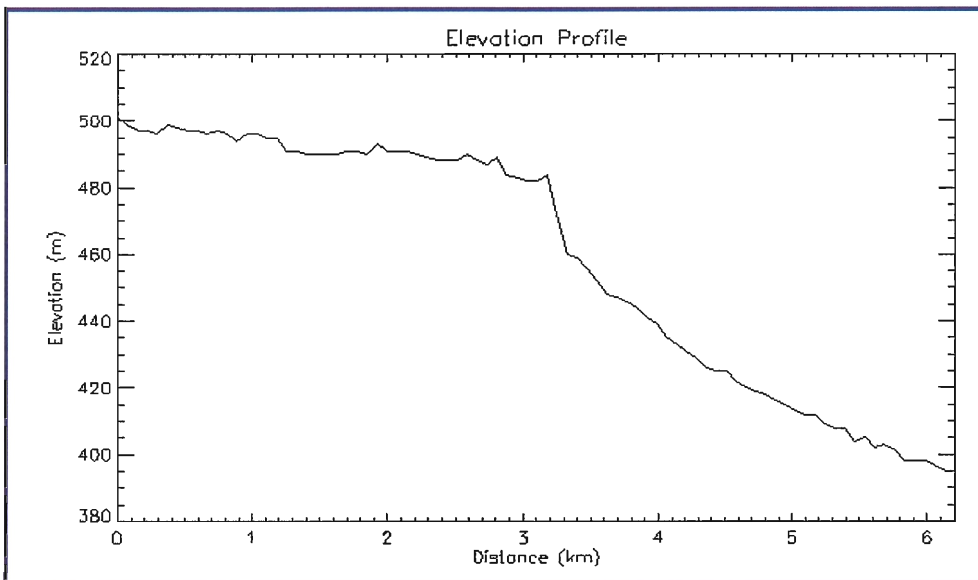
4.14 This profile is representative of the slope used in the second erosion model. This was designed to select a more constrained area over just the escarpment rise.
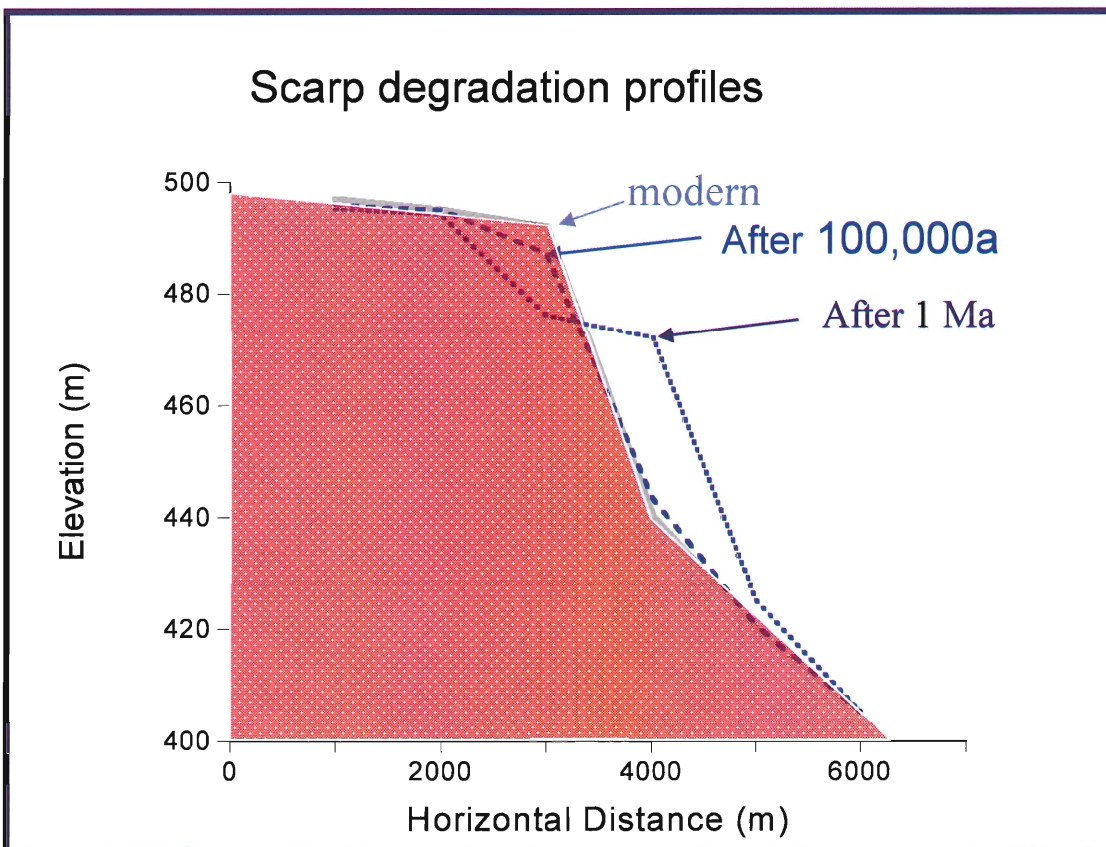
4.15 According to the diffusion model, this graph represents projected erosion rates over the face of the scarp over periods of 1000, 100,000, and 1m.y. While this does show the expected trend of slope equalization, once again this data can only be accepted as a possible general trend due to variables unaccounted for such as the cap rock.
($k = 1m^2/ky$)

The data provided from using the diffusion model on both the extent of the alluvial fan holding the scarp, and on the scarp face show the expected trend of small amounts of erosion lessening the slope of the landform over time. This is seen in the previous three figures, and most clearly represented in figure 4.15. Due to assigned boundaries of measurements, assigned k based on the environment, and the important presence of the cap, these models will be accepted as general trends only.

4.4 Long Profiles and assessment of knickpoint position

Patterns in the position of knickpoints on streams perpendicular to the scarp face can be useful in determining the genesis and evolution of the escarpment. Figure 4.16 shows the location of the first six selected channels. The channels do not appear to contain active streams but may be considered "washes" that intermittently may hold flood discharge. Figure 4.17 is the combination of these channels in long profile after being equalized according to distance from the escarpment. Because most potential knickpoints are located within 80km of the escarpment, a magnification of this region was stretched in the X axis, seen in figure 4.18. It is apparent in figure 4.16 that the occurrence of these channels can be defined in sets, with channels 6,5, and 4 running similar paths, channels 3 and 2 in a group, and channel 1 as an outlier. Notable among observed patterns of knickpoint propagation include the presence of many (up to 7) individual points on channels 2 and 3, with points often correlating with the other channel. Many of these points are spread out along the extent between the escarpment rise and up to 75km distant. Channels 5,6 and 7, show only 1 or 2 knickpoints each, all located very close to the initial escarpment rise. Channel 1, shows, like channels 2 and 3,

knickpoints spread over its extent, but fewer of them. This could be due to the low flow gradient, and possibly more evolved channel path of this outlying river. The most likely reason for anomalous data in this reason is the presence of Holocene basaltic flows across some regions, which could disrupt original flow paths (Nielson et al., 1999) .
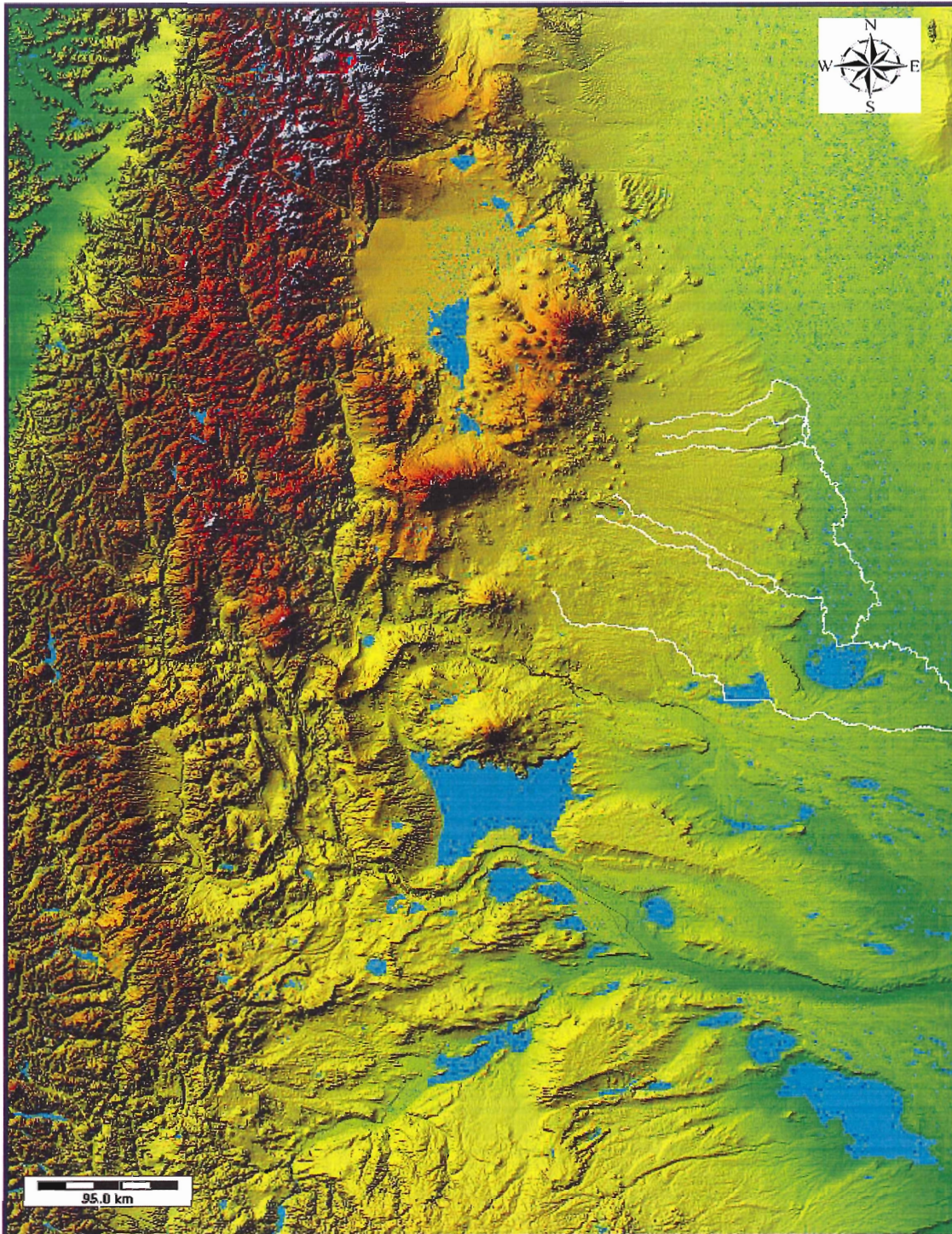
Figure 4.16 First selected six streams shown on Rivertools DEM.(From channel 1 to 6, moving from south to north. These channels were chosen on the basis that on first observation of their channel profiles in Rivertools they appeared to contain potential knickpoints.
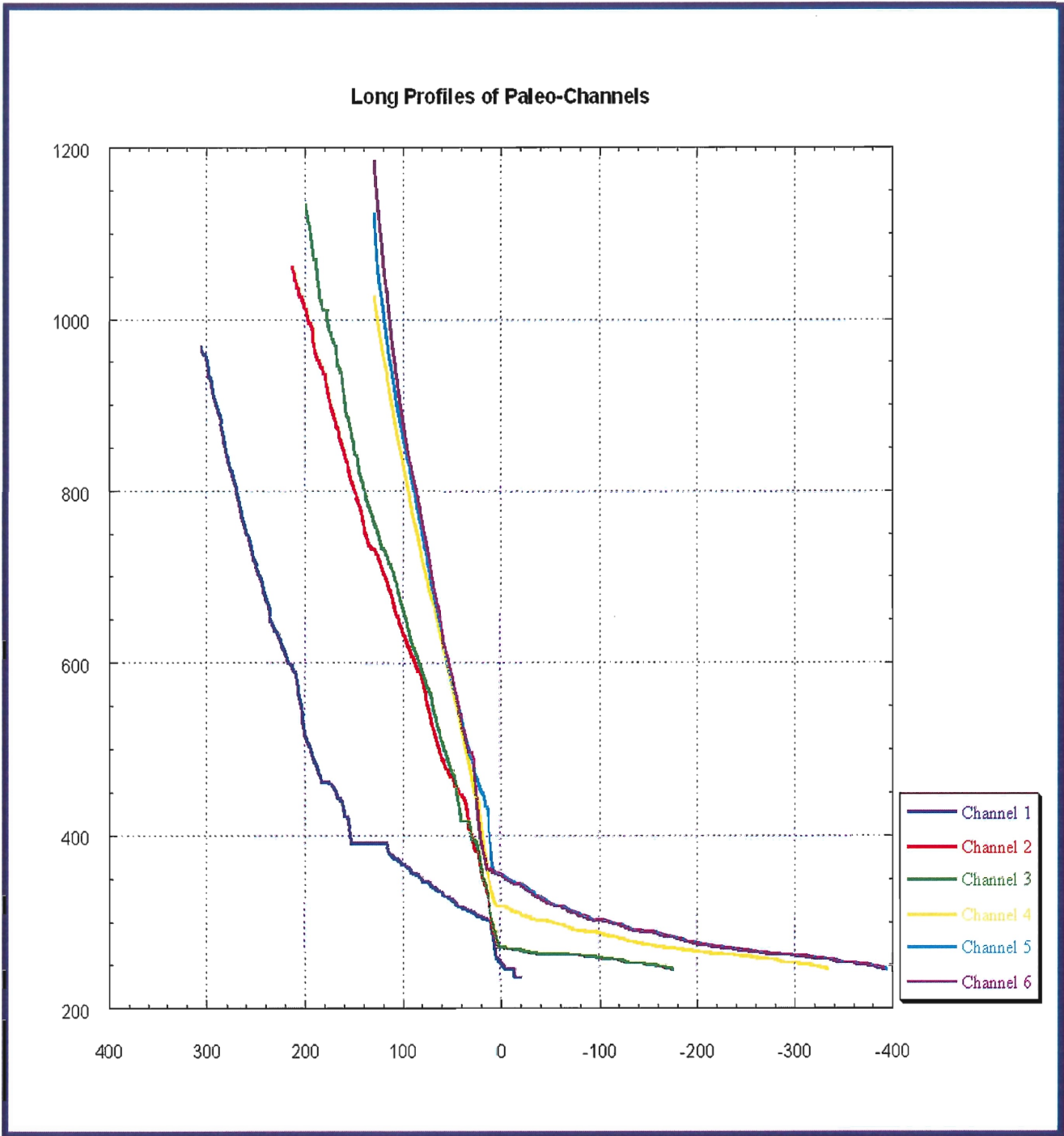
Figure 4.17 This figure shows the combined channel profiles of the six selected paleo channels. The grouping of channels 2 and 3, and 4,5, and 6 is apparent when they are graphed together. Channel one, an outlier, runs across a reservoir, giving the large flat surface at around 390m elevation.

Figure 4.18 This zoom of the boxed region of the paleo channel profiles shows a recognisable trend of greater kinckpoint presence and lateral propagation in the south as opposed to the north. Channel one is interpreted as somewhat anomalous due to the presence of some basalt flows overlying earlier channel deposits, however, it still shows more kinckpoints and lateral migration of the erosive zones than the channels to the

Long profiles of paleo-channels
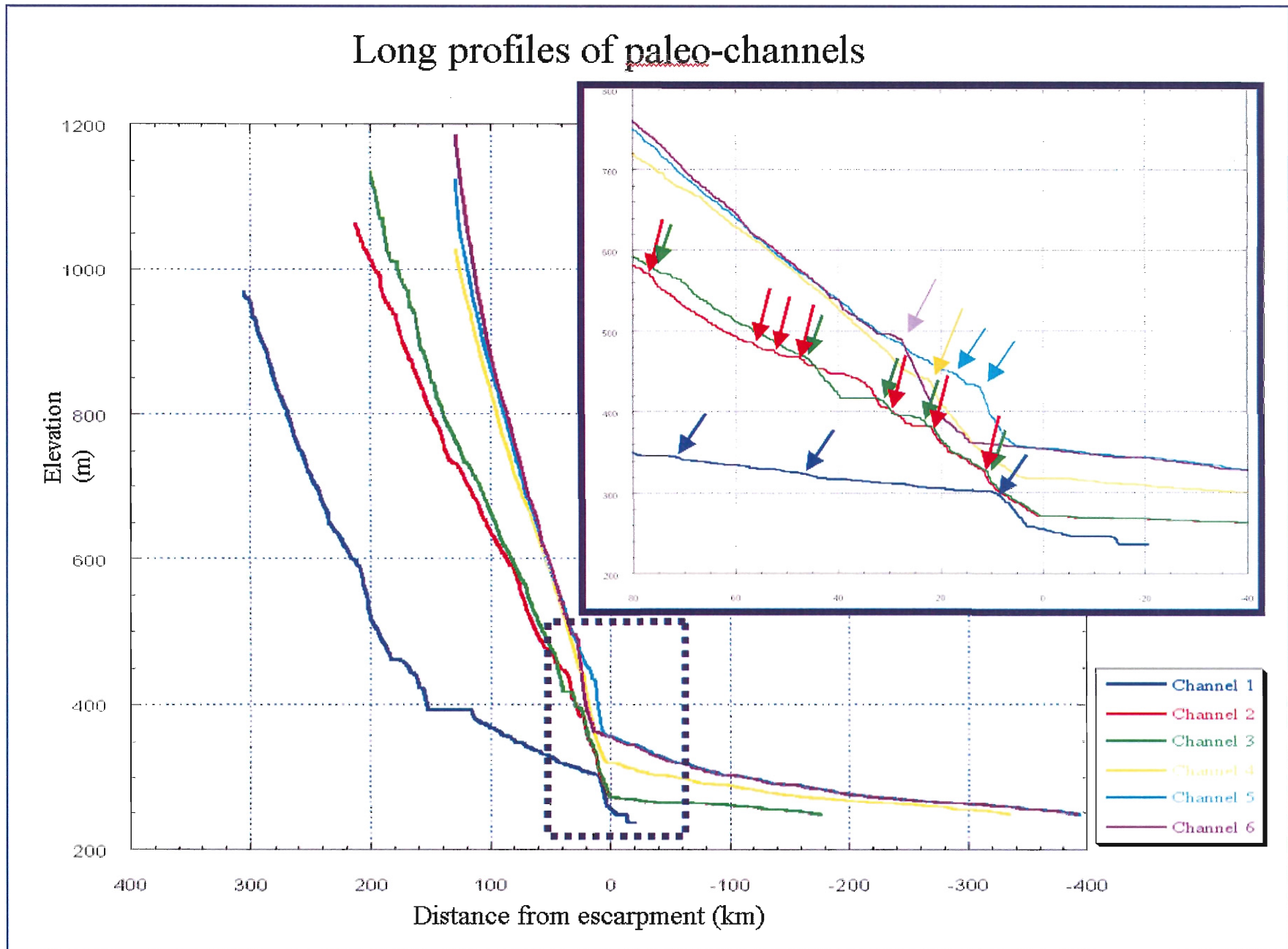
Upon observing this apparent trend of knickpoint frequency and greater propagation in channels to the south over the north, six similar channels were selected to attempt to confirm this trend. Figures 4.20 through 4.23 represent southern channels, while figures 4.24 though 4.26 depict more northerly routes. These channels in comparison show an obvious pattern in both presence and propagation of knickpoints, as well as slope and length. The southern group shows between 3-5 possible knickpoints per channel, each spread through the channel length. The northern channels show at most 1-2 definable knickpoints, all located in close proximity to the escarpment rise. In general, these profiles also tend to have greater slopes, and smoother profiles in comparison with the other channels. Though there is a strong similarity and overlap of channels plotted by rivertools, the six channels in figure 4.19 were selected based on variation (in some cases quite slight), trend, and the lack of possible interfering factors such as sporadic volcanics. There are no mappable channels present in the central region of the complex. In the following figures (4.20- 4.26), as in the previous channel set, the criteria used to define a knickpoint includes firstly the basic identification; if the slope line of the high point is extended, it must be significantly different than the given stream slope. Also, surrounding factors such as volcanism, watersheds, and faulting must be considered, as they can produce sharp anomalies similar to the expected profile of a knickpoint.
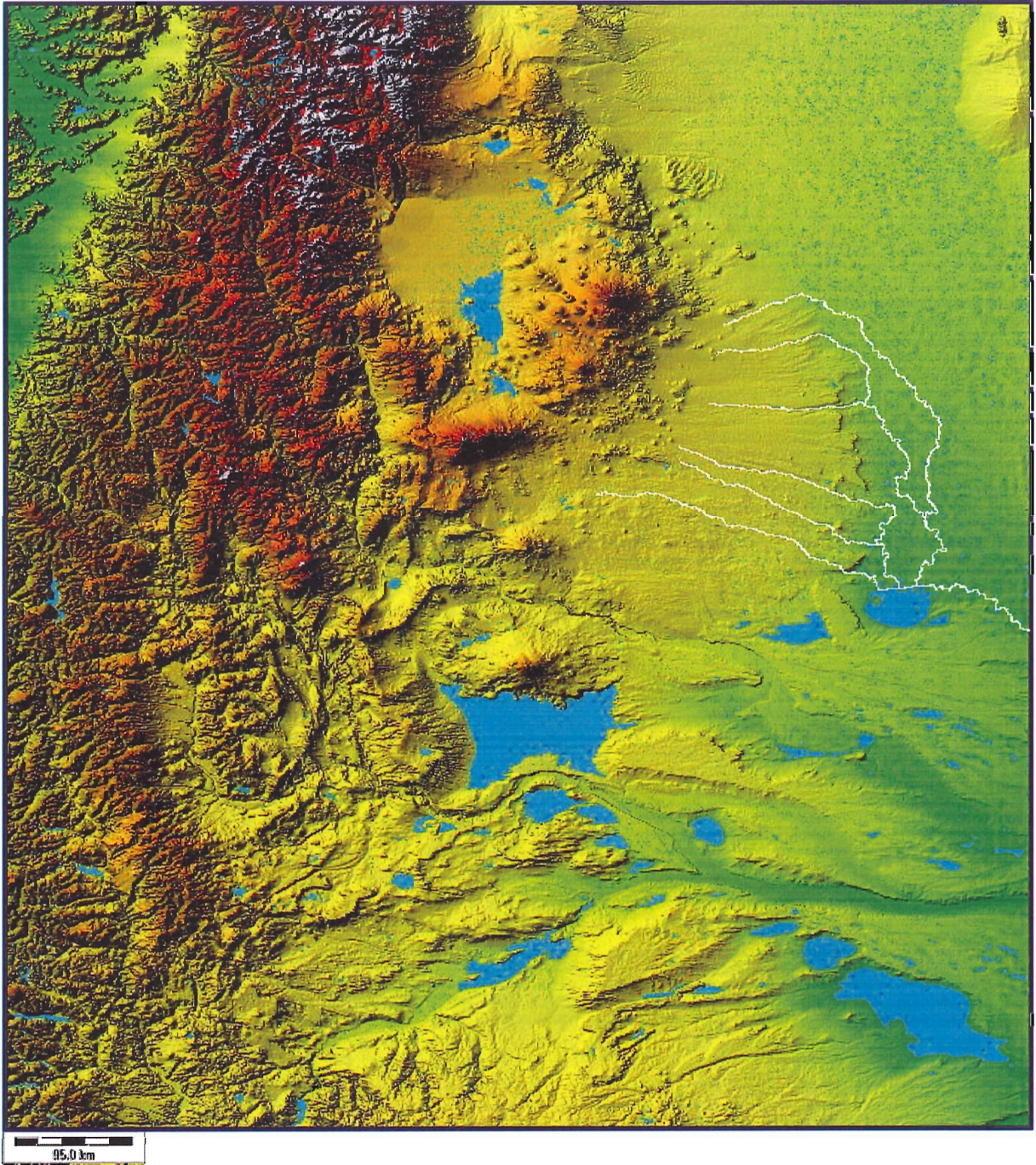
Figure 4.19 The second set of six channels were selected again based on the likelihood that that may as well contain knickpoints, and were also used to compare the new profiles with the older data. These channels were also examined in terms of their entire long profiles, as opposed to focusing solely on the scarp face region.
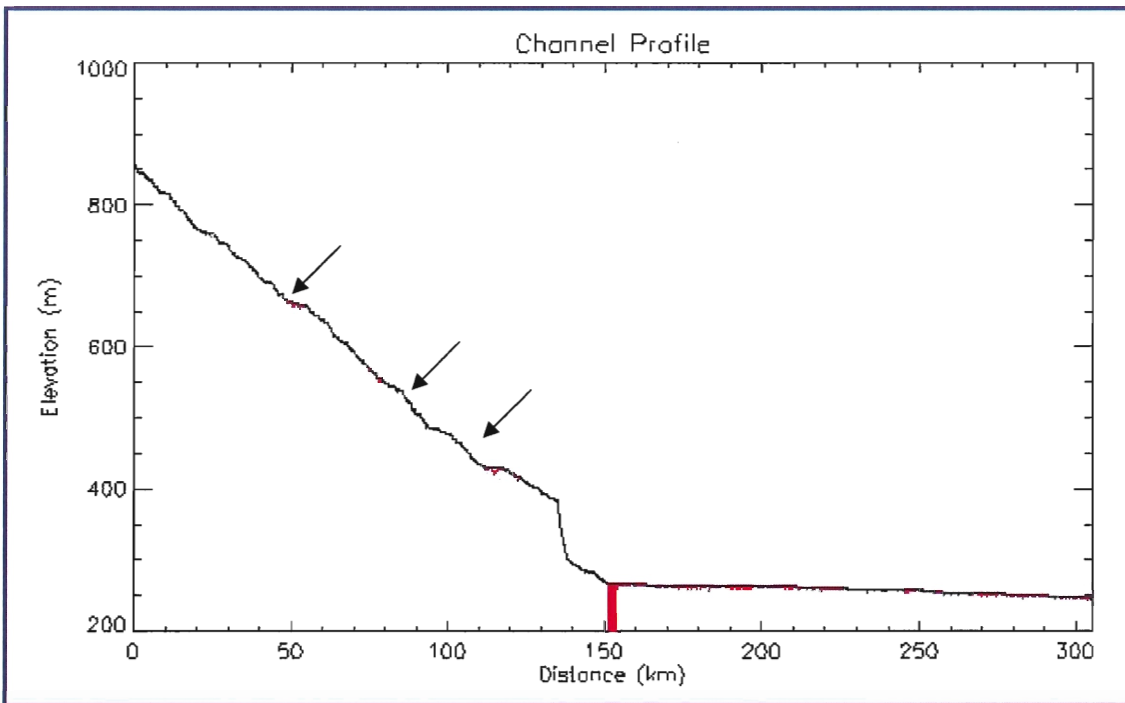
Figure 4.20 Southernmost channel (Channel 1b) again shows multiple knickpoints propagating over 100 km along the escarpment rise.
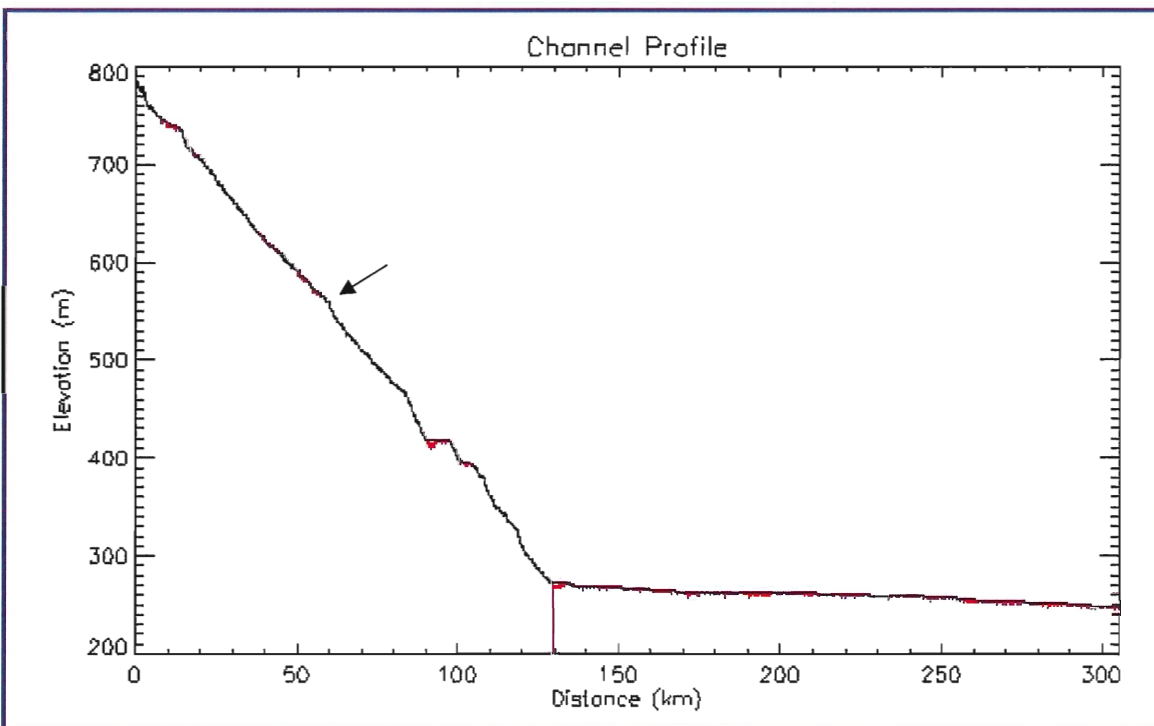
Figure 4.21 Channel 2b shows one distinct knickpoint, and may hold others between 100 km and the rise, but the profile has been distorted due to the presence of a reservoir seen between 90 and 100 km.
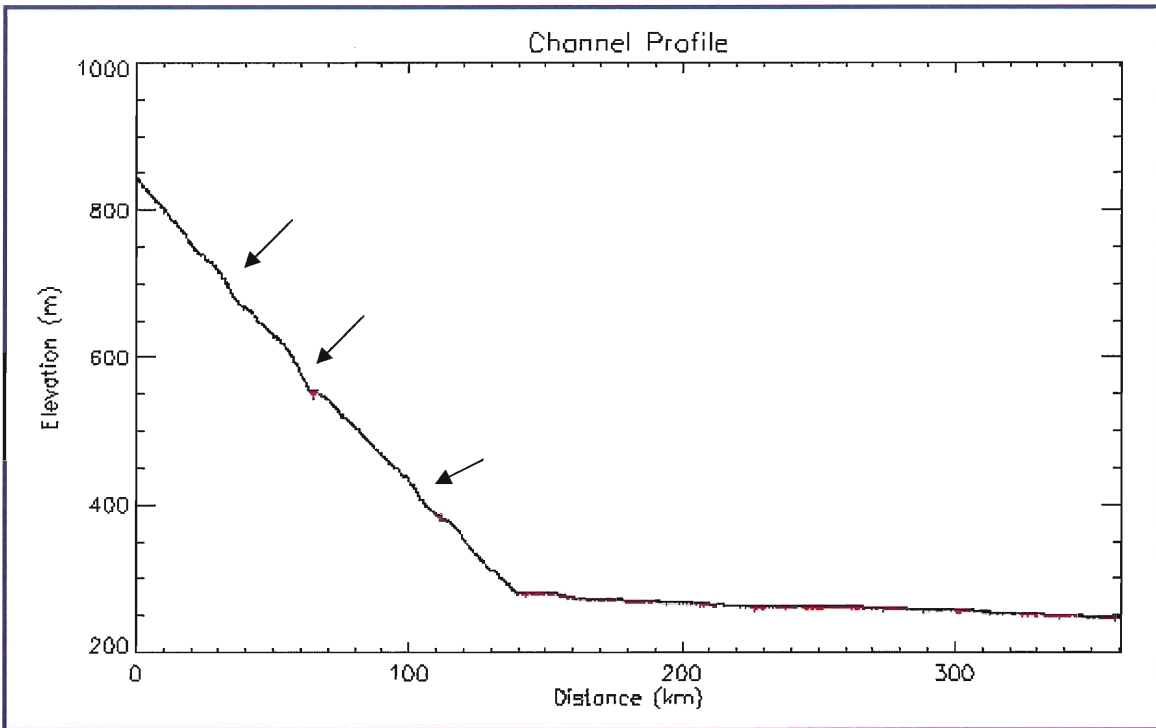
Figure 4.22 Channel 3b shows 3 notable knickpoints along its extent.
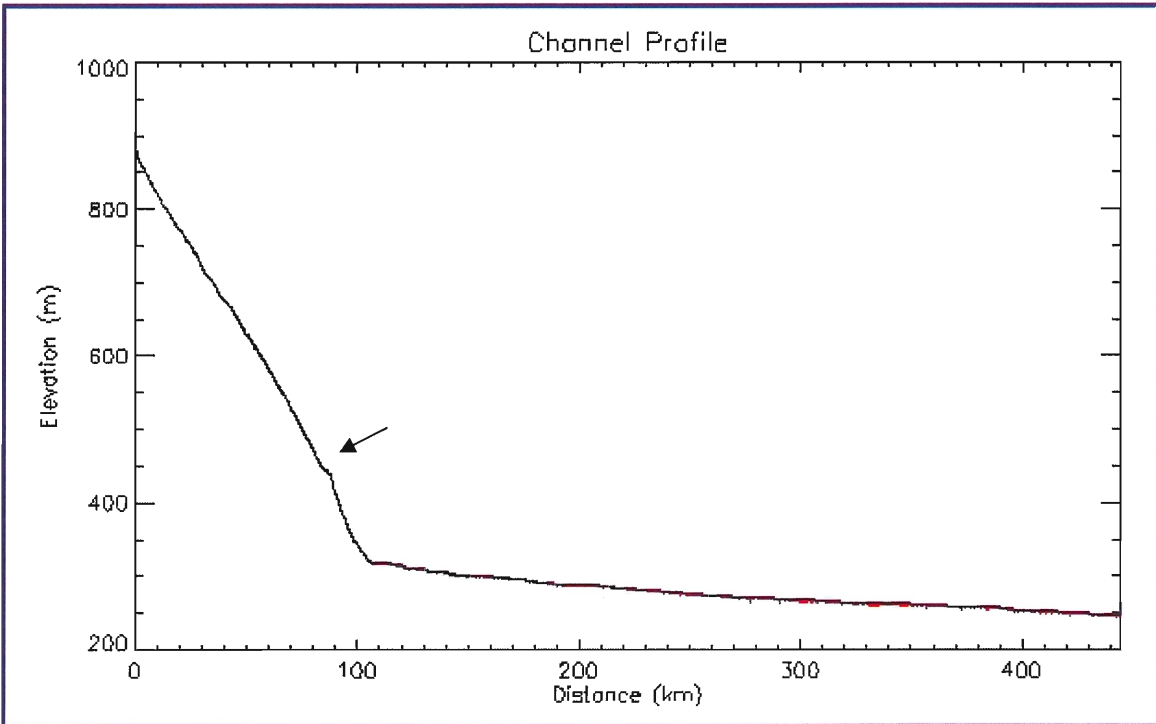
Figure 4.23 Channel 4b shows only one knickpoint, just above the escarpment face. This is in keeping with the expected pattern from the first channel set.
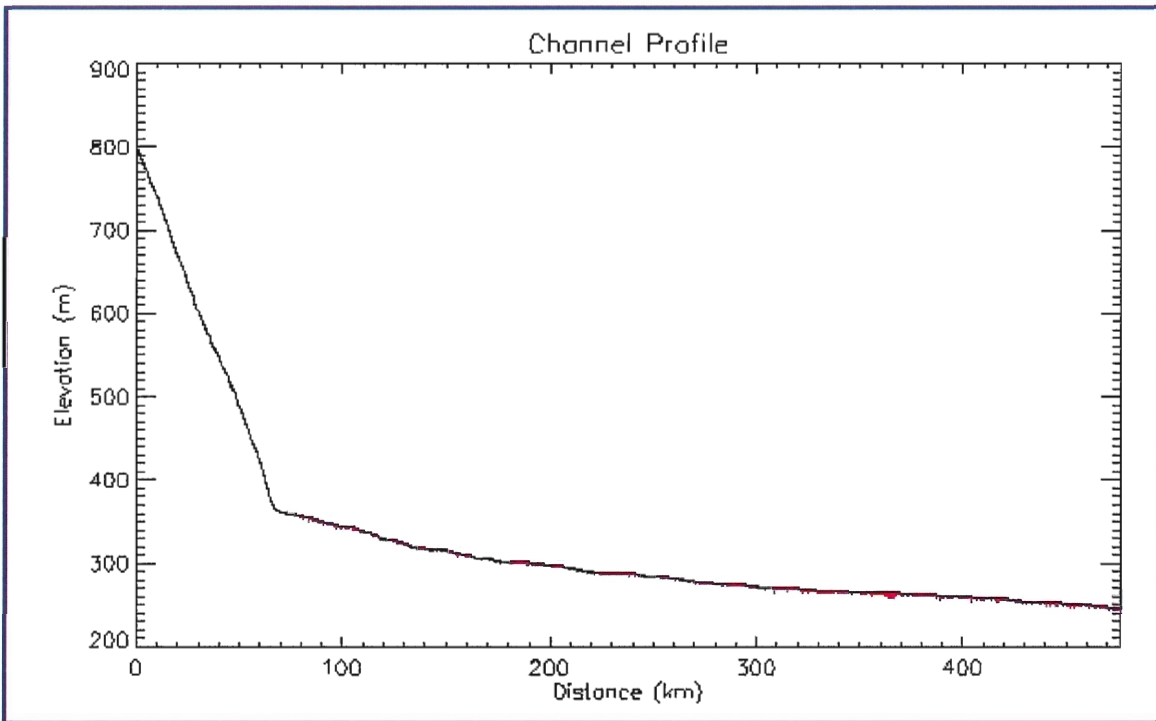
Figure 4.24 Channel 5b shows no knickpoints.
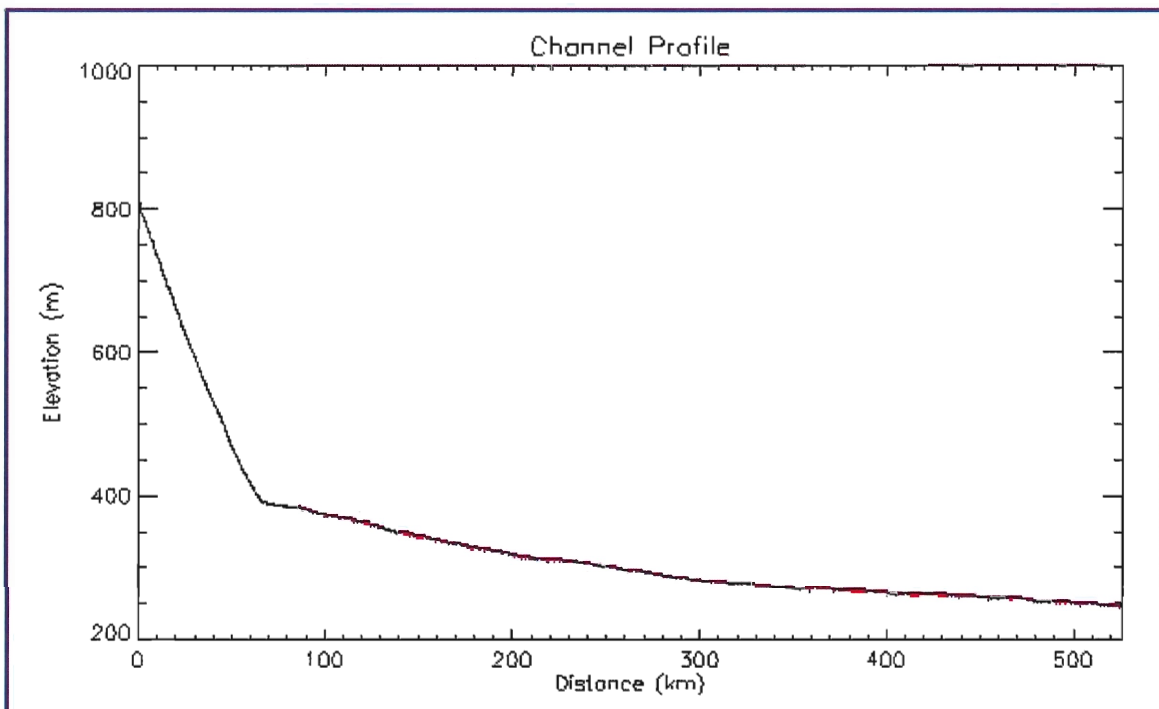
Figure 4.25 Channel 6b shows no knickpoints, as expected according to channel set 1.

Finally, the channel profile of the Rio Salado, running parallel to the escarpment,

is seen in figure 4.27 and 4.28.
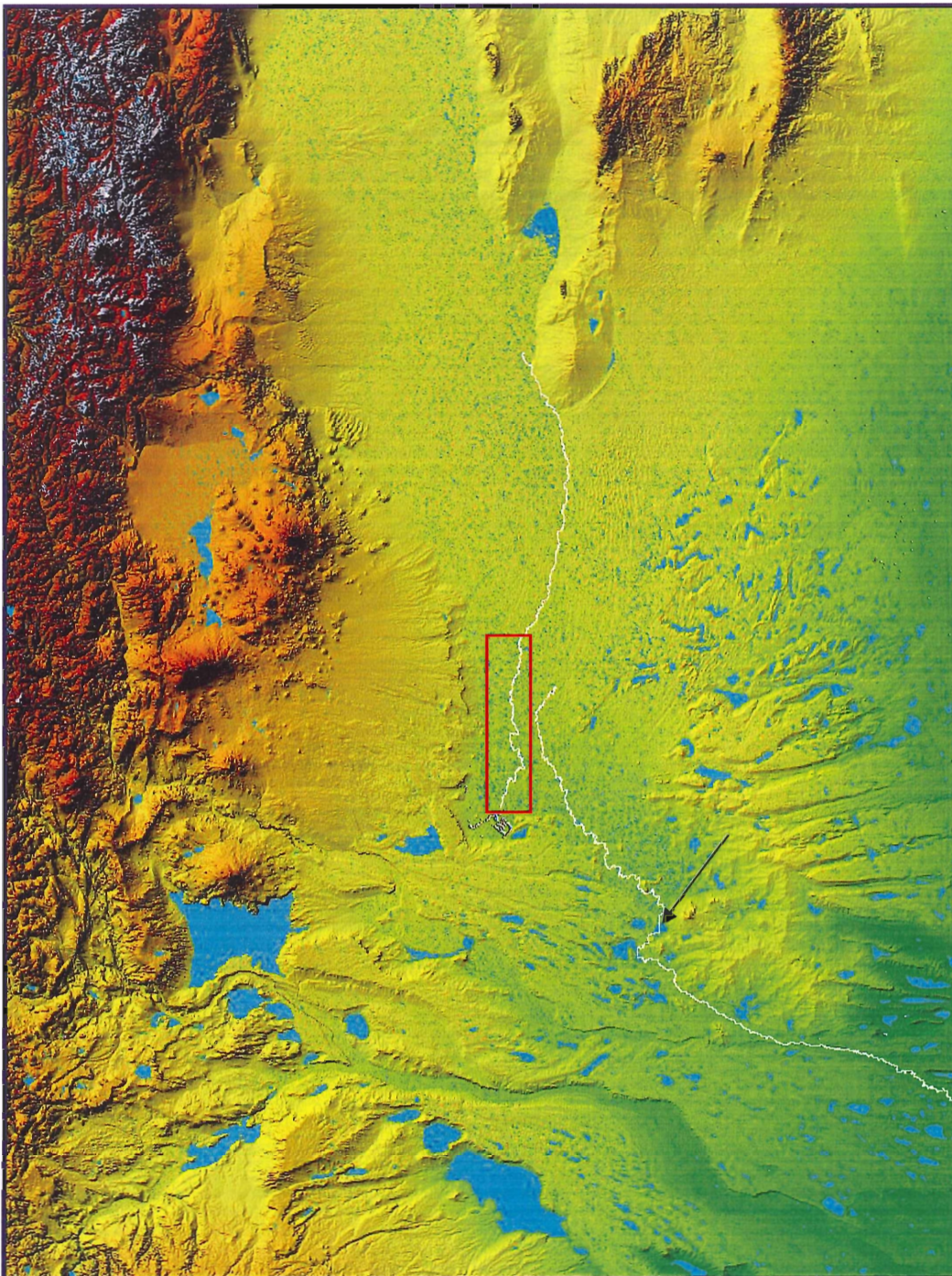
Figure 4.26 The Rio Salado. The disjoin is the result of a gap in the SRTM data at the base of the northern reach being interpreted by Rivertools. The flowpath is joined based on geologic and topographic maps. The red box indicates the knickzone shown in the channel profile of figure 4.27). Approximately at the arrow the river experiences a significant base level change (figure 4.28).
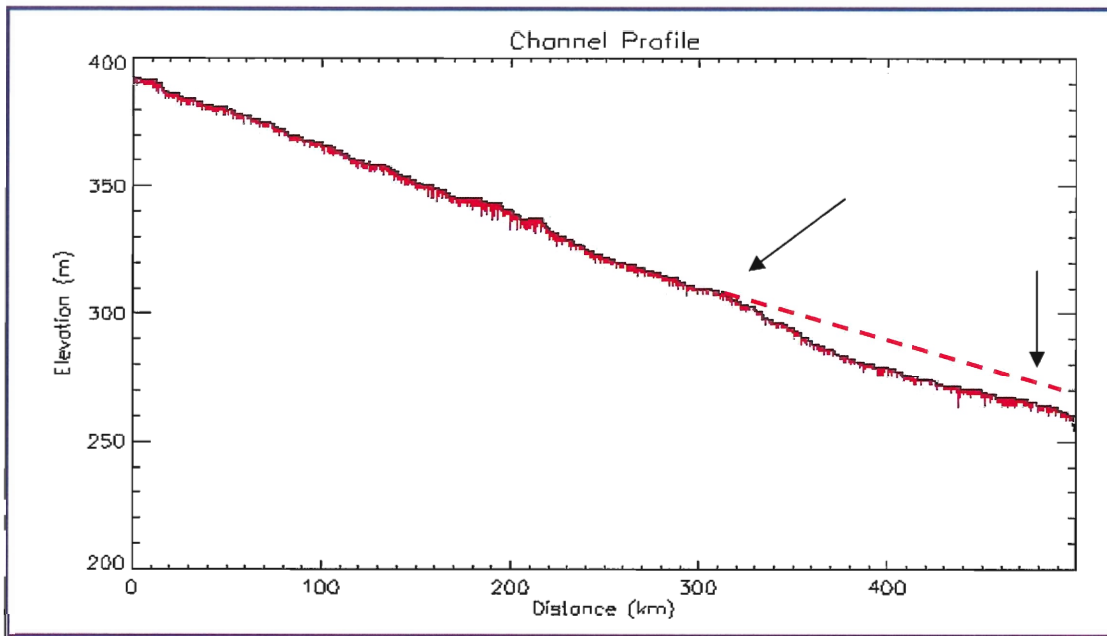
Figure 4.27 The northern profile of the Rio Salado. The original flow path is extrapolated in the red dashed line. The knickzone is marked at both extents by the arrows. This zone, extending almost 200 km, is roughly indicated on the DEM in figure 4.14.
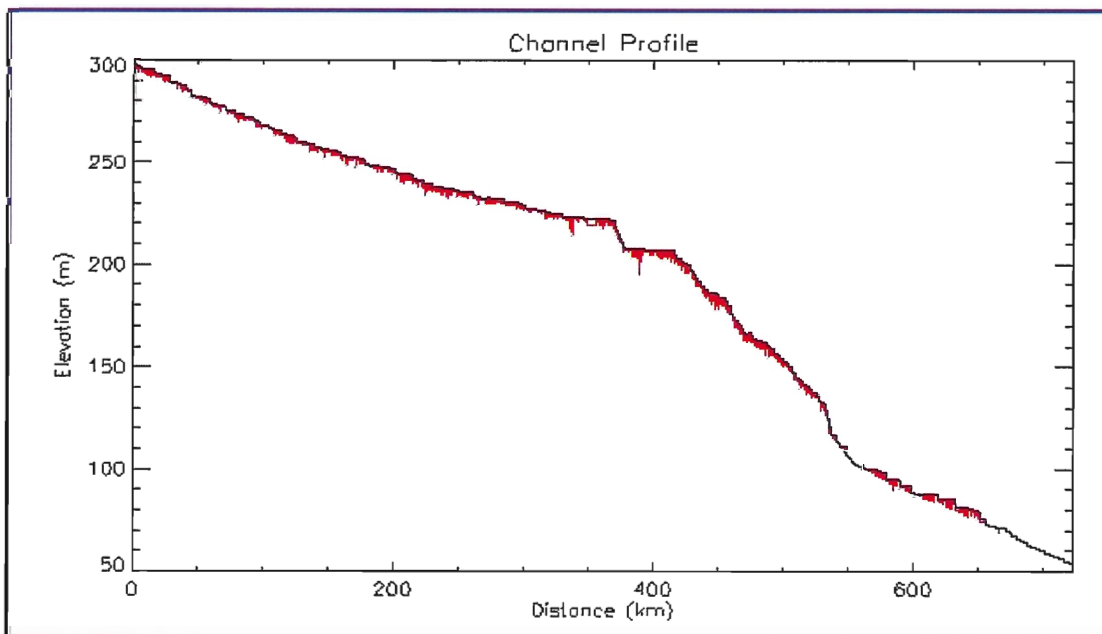
Figure 4.28 The southern profile of the Rio Salado. At about 350 km the river experiences a sharp drop, which roughly correlates with the location of fault events in the region. It then crosses a reservoir and proceeds down a very steeply graded slope. This change in base level could potentially be the cause of the knickpoint to the north.

4.5 Evolution of the carbonate cap

The extent of the carbonate cap (dated as middle Pliocene by Nielson et al., 1999) is currently mapped based on the visible occurrences in highly weathered and exposed areas such as the steepest escarpment faces, and the vertical fault cuts in the alluvial surfaces found directly to the east. The location of mapped carbonate deposits of the mid-Pliocene are shown in figure 4.29 to cover both the outer exposed upper surface of the escarpment, and the eroded faces of similar elevation in the remnants of the alluvial fan directly to the east. The escarpment carbonate is overlain by further alluvial deposits from the west, while the easterly fan is overlain by eolian deposits. The relationship between these landforms in elevation profile is shown in figure 4.30. The greater slope of the escarpment could partially be explained by the vertical exaggeration of the image, and by a larger amount of fluvial deposition accumulating material above its carbonate cap. The lower elevation alluvial fan is likely at its height because the addition of further eolian sediments(Nielson et al., 1999) has been relatively little in comparison. The cap itself is about 3m thick, and the overlying material on this formation is described as fine grained, silty eolian sediment (Nielson et al., 1999; field observations by J Gosse, personal communication, 2007). With this information it is possible to extrapolate the potential locations of either the alluvial mega-fan, or system of large fans which have created these landforms.
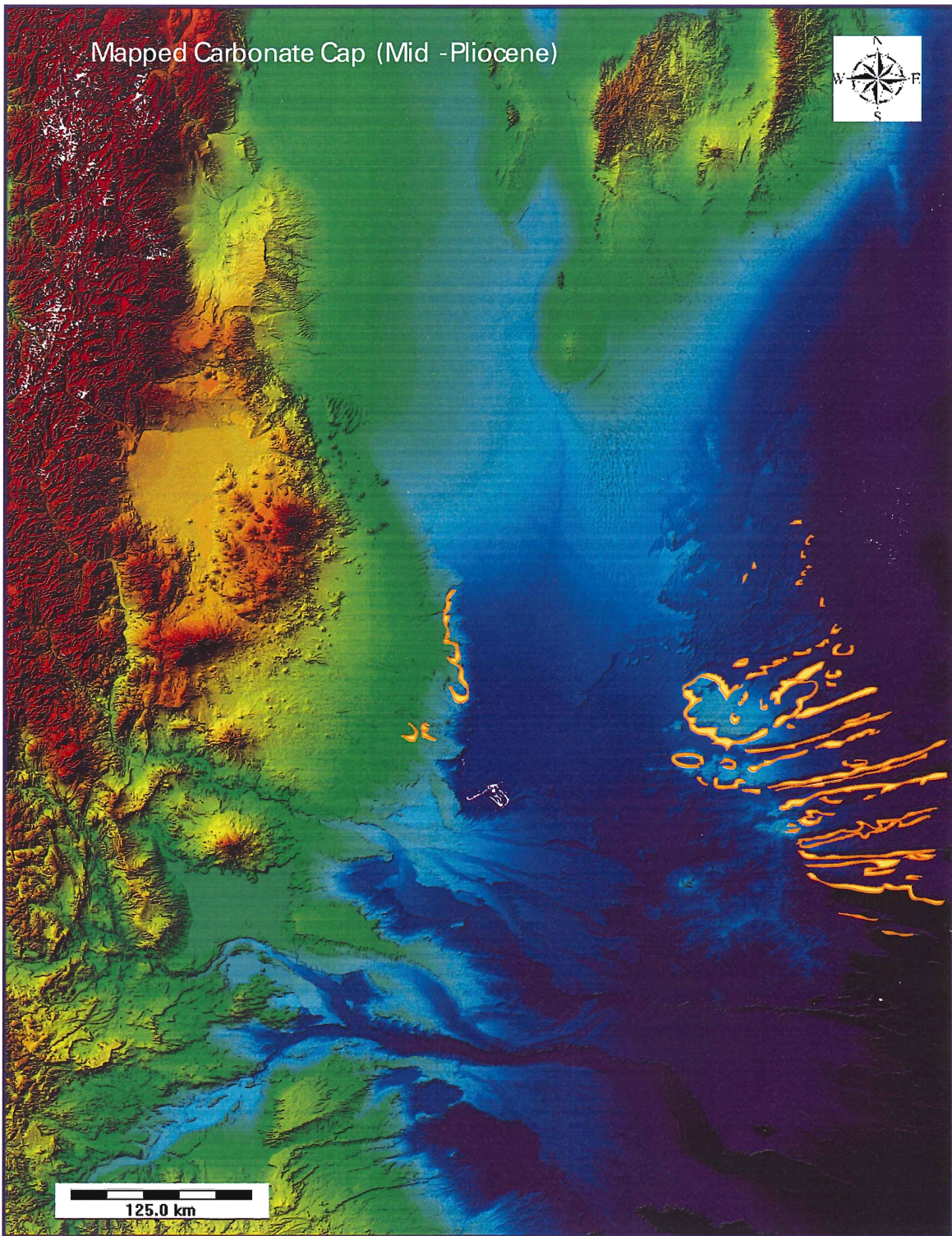
Figure 4.29 The mapped extent of the carbonate cap according to Nielson et al., 1999. This figure is meant to demonstrate the correlation between the alluvial fan preserved in the east, with the carbonate capped escarpment of the same age on the west.
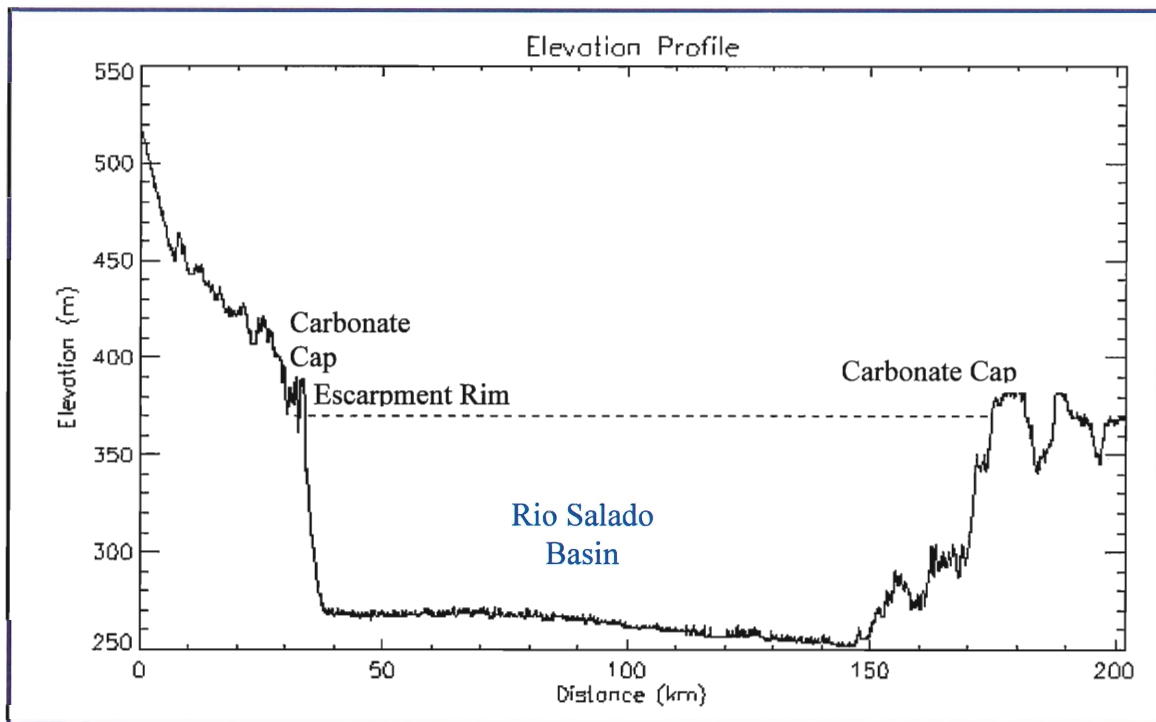
Figure 4.30. This elevation profile shows the topographic relationship between the escarpment and the alluvial fan in the east. Note the similar elevation rise of over 100m and the well preserved faces due to the carbonate cap.

Figure 4.31 Field photograph of the 3m carbonate cap overlying the Santa Isabelle escarpment. Note the extremely well preserved, flat top.

Chapter 5.0 Interpretation

5.1 Evidence for fluvial origin of the escarpment

Perhaps the most compelling geomorphic evidence for fluvial influences on the Santa Isabelle escarpment are the multiple indications of unusual erosion patterns moving from the south to the north. This is indicated by the varying levels in sinuosity along the lateral extent of the escarpment, by the differences between elevation profiles across the scarp in representative regions, and through uneven incision rates of fluvial knickpoints. The elevation profiles in the north show a shallow slope gradient, while the central and southern slopes both contain well defined scarp faces. This suggests that the greatest amount, or newest cutting erosion has taken place in the south and central regions, while the north has remained relatively uncut. The measured sinuosity of the escarpment differs from an average of 1.6 in the centre, to 1.2 in the north, which also implies uneven erosional influences. The highest levels found in the central region suggests the largest amount of erosion occurred in this area, while the lower levels towards the north imply less exposure to erosional forces. This pattern, confirmed by the topographic profiles showing defined scarp slopes in the central region and shallow gradients in the north, suggests an dominant erosive force propagating from the south east.

Based on the observed pattern that river channels on the southern slopes of the escarpment contain far more knickpoints which have advanced as far as 180 km upstream, contrasting with the northern channels containing an average of one knickpoint (which is typically located within a few kilometers of the escarpment rise) it is again likely that the erosional force propagated in a non linear fashion from the south. The uneven distribution of kickpoints also serves to rule out faulting as the primary cause of

formation, leaving the possibility that this is a fault scarp ruled as unlikely. The correlation between the Rio Salado's large knickzone and the frequency and magnitude of knickpoints in the escarpment channels is a conclusive indicator that these forces are directly related. This relationship involves the headward erosion of the Rio Salado due to base level change, which in turn causes increases in magnitude of erosion and incision on the escarpment. This type of migration would also therefore serve to explain the variation in levels of sinuosity over the escarpment

5.2 Evidence for tectonic origin

In relation to this landform being a fault line scarp, although there is significant evidence in both mapped faults and displaced geomorphic surfaces of notable large scale in the area, none of the currently mapped faults or evidence of faulting appear to correlate directly with the scarp formation. Given this evidence and the supporting data from knickpoint analysis, the most significant observation related to faulting events is that the major rivers in the area appear to follow the larger faults. This suggests that though the Santa Isabel escarpment may not directly be the result of a fault, the faults may have provided flow paths for the river which could have caused significant erosion of this landform. Faulting may also be the mechanism responsible for the base level change in the gradient of the Rio Salado, causing the generation of the rivers knickzone and subsequent knickpoint formation in the escarpment channels. Some of the changes in sinuosity of the escarpment, namely the anomalous zones of low (1.05- 1.00) readings, may also be attributed to small scale fault events. The northern graben, and southern displaced block are prime examples that faults occur on a small scale along the scarp face.

5.3 Further Considerations

The mapped extent of the carbonate cap indicates that one or more alluvial mega fans deposited mass amounts of material over the Pliocene period, which later formed a pedogenic carbonate cap on top of the deposits. The elevation profile, which indicates a comparable rise cut by deep incision of both the escarpment and the eastern alluvial fan suggests a similar formational event. It is also possible to extrapolate that the carbonate cover is much more extensive than is visible, and it may underlie much of the subsequently deposited alluvium and eolian sediment. In comparing the available geologic maps, it can be determined that some of the uneven slope and channel readings given from the southern extent of the escarpment can be attributed to various basaltic flows related to the volcanism in the west. The mapped pediment which formed as a result of deposition from the Rio Salado (Nielson et al., 1999), is also observed to extend to the base of the escarpment, suggesting a previous route which brought the channel even closer to the escarpment.

5.4 Proposed model of the formation of the Santa Isabel escarpment.

Given these results, a potential model of the formation and evolution of the Santa Isabel escarpment has been formed. This model is also represented in figure 5.2, which shows the formational events in order. Figure 5.1 is a representation of the basic formation of an alluvial fan, or fan complex. The initial traceable event is the mass deposition of alluvial sediments in the entire region of the study area. This material would have likely originated from the Andes in the west, and would have covered at least the

extent of the escarpment to the end regions of the western alluvial fan. Following this deposition, there was an increase of volcanic activity during through the Pleistocene. This change in environment may have caused a hiatus in fluvial deposition, which caused the starvation of the previous depositional surfaces. The semi arid climate at the time would have been conducive to the formation of the pedogenic carbonate cap on the surface of the remaining landforms. Eventually, regional faulting would cause re-direction of the local river systems, primarily the Rio Salado. A major change in base level would add to the erosional force of this river, allowing for significant incision of the area in the centre of the escarpment and the alluvial fan. The movement of the river towards the escarpment would cause the steep undercutting of the rise, while the headward movement of the Rio Salado knickzone would drive the propagation of the knickpoints of smaller order channels along the escarpment. This movement would result in the changes in sinuosity and slope across the N-S range of the landform. Subsequent fluvial deposition along the escarpment would serve to increase the slope, as well as overlay the carbonate. Thinner eolian deposits would overly the capped fan to the east. The carbonate caps on both extents would of course play a large role in the preservation of the vertical rise of the landform as fluvial erosion continued to undercut the region.
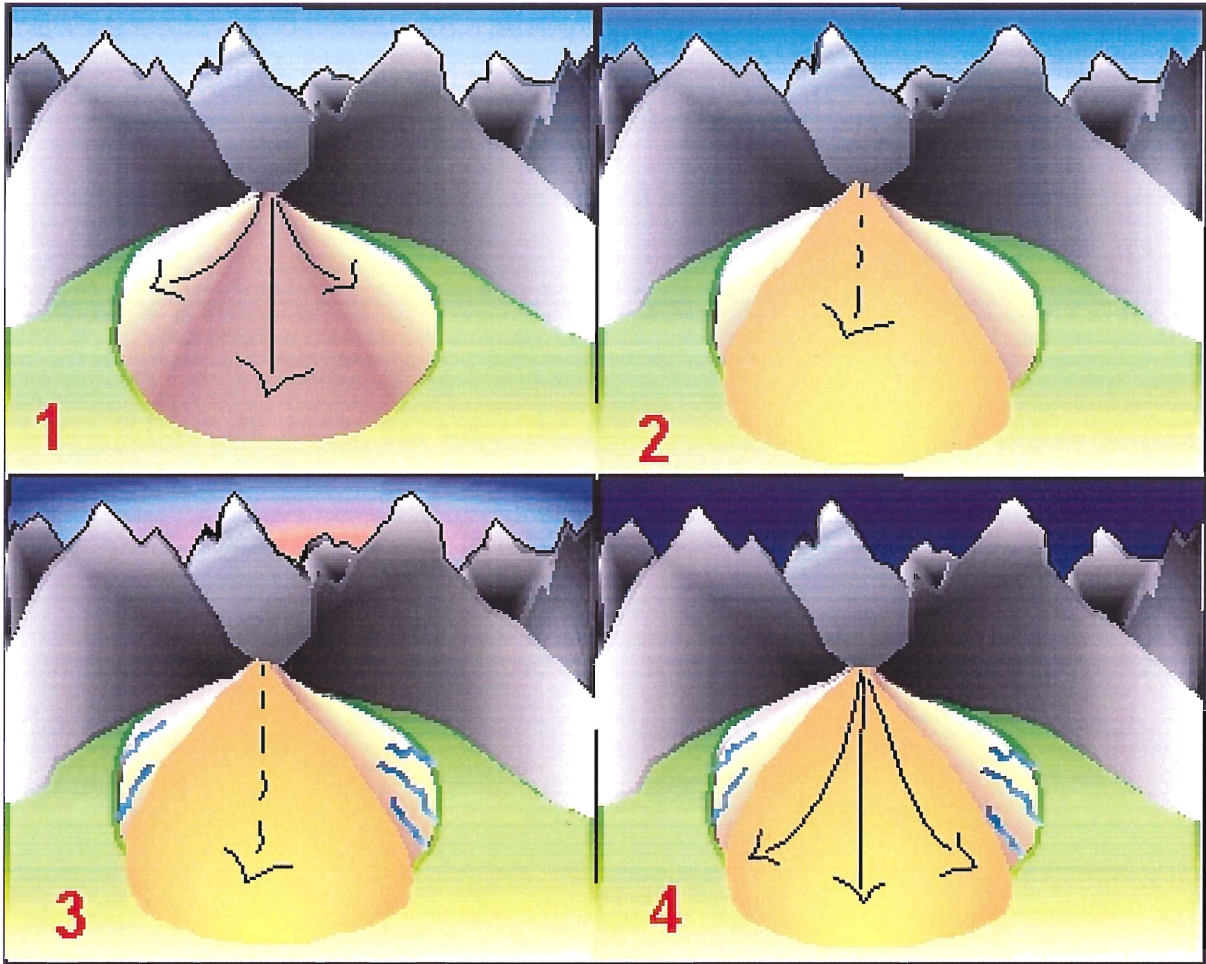
Figure 5.1 The stages of alluvial fan formation: a) initial spreading and building of the fan across a mountain piedmont b) fan build up along central plane, or degradation in central region according to changes in environment. c) erosion and gully formation of older material d) further pulses of aggregation deposition along the central region.(Interpreted based on relationships shown in figure 2.0 from Hsu and Pelletier., 2003.)
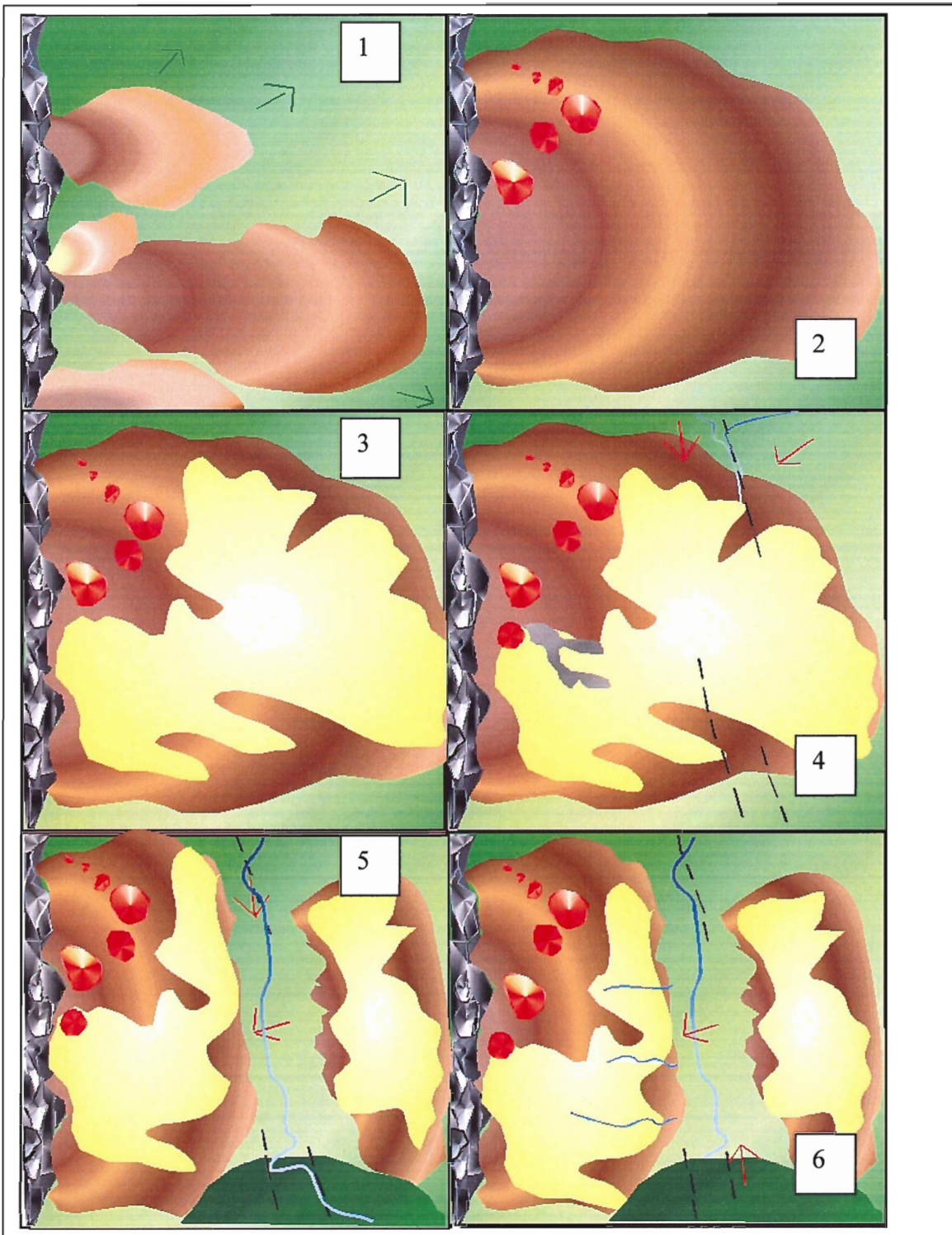
Figure 5.2 A proposed model for the formation of the Santa Isabel escarpment (The Andes mountains are shown in grey on the left) : 1) The deposition of alluvial material on the plains east of the Andes range 2) The initiation of volcanic activity on the complex 3) The formation of the carbonate cap 4) Faulting causing redirection of rivers and southward erosion. Basaltic deposition 5) Base level change, increased erosion parallel and cutting into the escarpment due to the movement of the Rio Salado 6) Knickpoint migration of channels on the Santa Isabelle escarpment as a result of knickzone propagation of the Rio Salado.

Chapter 6.0 Conclusion

Based on available and reasonably extrapolated data, it is suggested that the Santa Isabel escarpment has formed though no one mechanism defined in the initial hypothesis, but rather through a combination of these influences over time. The primary mechanism which caused the erosion and formation of this escarpment is fluvial incision, which was initiated and driven by faulting events and base level change. Based on the proposed model of formation, the escarpment face is the same age or younger than most of the volcanic features, and formed concurrently with the incision of the Rio Salado and associated evolving channel bodies.

6.1 Sources of error

Because the vast majority of this work was conducted remotely, it was not possible to verify many interpretations though field work, nor was it possible to identify underlying material in many cases, which could potentially lead to errors in interpretation. In modeling the erosion of the escarpment, the data was not applied in the interpretation and conclusion because the error in this method was deemed too great due to variables which may either be inaccurate (k) or unaccounted for (the protective cap).

6.2 Suggestions for future work

Future work on the escarpment could include detailed stratigraphic analysis of the units of the scarp (landform and face), including observation of possible flow patterns, and stratigraphic progression. Field and petrographic work with U-series dating could confirm whether the carbonate cap is pedogenic, and whether the caps on the Santa Isabel escarpment and the eastern alluvial fan are of the same age. Locations of faults and mapped seismic events according to magnitude could be used to infer tectonic activity in

relation to landform formation. The cause of the base level change of the Rio Salado is a question that could likely be answered using similar methods to this project, extending the DEM range and study area to the coast, and comparing the migration pattern of the river's knickzones as it connects with the Rio Colorado.

Refrences

Allmendinger, R. W., Ramos, V. A., Jordan, T. E., Palma, M., and Isacks, B. L., 1983, Paleogeography and Andean structural geometry, northwest Argentina: Tectonics, v. 2, no. 1, p. 1-16.

Baker, Sophie E, 2005, The Quaternary History of the Rio Diamante, Mendoza Province, Argentina.Dalhousie University. p. 17-43.

Baldauf, P. E., 1997, Timing of the uplift of the Cordillera Principal, Mendoza Province, Argentina [PhD thesis]: The George Washington University, 356 p.

Bull, w., 1991, Geomorphic Responses to Climatic Change, Oxford University Press, p3-7.

Gardner, T.W., Jorgensen, D.W., Shuman, C., and Lemieuz, C.R., 1987, Geomorphoc and tectonic process rates: Effects of measured time interval: Geology, v.15,p.259-261.

Giambiagi, L. B., Alvarez, P. P., Godoy, E., and Ramos, V. A., 2003a, The control of preexisting extensional structures on the evolution of the southern sector of the Aconcagua fold and thrust belt, southern Andes: Tectonophysics, v. 369, p. 1-19.

Gosse, 2007. Personal Communication on field observations, sample colllection and photography.

Hsu, L. and Pelletier, J.D., 2004, Correlation and dating of Quaternary alluvial-fan surfaces using scarp diffusion: Geomorphology 60, p.319-335.

Introcaso, A., Pacino, M. C., and Fraga, H., 1992, Gravity, isostasy and Andean crustal shortening bet ween latitudes 30 and 35 degrees south: Tectonophysics, v. 205, p. 31-48.

Jordan, T. E., Isacks, B. L., Allmendinger, R. W., Brewer, J. A., Ramos, V. A., and Ando, C. J., 1983, Andean tectonics related to geometry of subducted Nazca plate: Geological Society of America Bulletin, v. 94, p. 341-361.

Kennan, L., 2000, Large-scale geomorphology of the Andes: interrelationships of tectonics, magmatism and climate, *in* Summerfield, M. A., ed., Geomorphology and global tectonics, John Wiley & Sons Ltd, p. 167-199.

Lavenu, A., and Cembrano, J., 1999, Compressional- and transpressional-stress pattern for Pliocene and Quaternary brittle deformation in fore-arc and intra-arc zones (Andes of Central and Southern Chile): Journal of Structural Geology, v. 21, p. 1669-1691.

McIntosh, J.J., 2004, Analysis of range-scale topographic changes from digital topography in the southern-central Andes (latitudes 32° to 39° S) [B.Sc.Honours thesis]: Dalhousie University.

Montgomery, D. R., Balco, G., and Willett, S. D., 2001, Climate, tectonics, and the morphology of the Andes: Geology, v. 29, no. 7, p. 579-589

Nash, D.B., 1974, The Relative Age of the Escarpments in the Martian Polar Laminated Terrain Based on Morphology: Department of Geology and Mineralogy, University of Michigan, Icarus 22, p 385-396.

Nielson, H., et al., 1999 Mappa Geologica de la provincia de La Pampa, Republica Argentina: Ministerio de Economia y Obras y Sercoios Publicos. Escala 1:750,000

Nullo, F.E.,1993 Mappo Geologico de La provincial de Mendoza, Republica Argentina: Misiterio de Economia y Obras y Sercoios Publicos. Escala 1:500,000.

Polanski,J., 1964, Descripcion geologica de la hoja 26c (La Tosca), Provincia de Mendoza, Servicio Geologica Nacional, Buenos Aires, 86p.

Ramos, V. A., and Kay, S. M., 1991, Triassic rifting and associated basalts in the Cuyo basin, central Argentina, *in* Harmon, R. S., and Rapela, C. W., eds., Andean magmatism and its tectonic setting: Geological Society of America Special Paper265: Boulder, Colorado.

Scholle,P., Ulmer-Scholle, D., 2003, A Colour Guide to the Petrography of Carbonate Rocks: grains, textures, porosity, diagenisis: American Association of Petrolem Geologists.

Ritter, D.F., Kochel, R.C, and Miller, J.R., 1995, Process Geomorpholgy, Oxford University Press, 3rd ed,p225-226

Yanez, G.A., Ranero, C.R., von Huene, R., and Diaz, J., 2001, Magnetic anomaly inyerpretation across the southern central Andes (32°-34° south): The rols of the Juan Fernandez Ridge in the late Tertiary evolution of the margin: Journal of Geophysical Research, v.106,no.B4,p.6325-6345

Zaprowski, B. J., Evenson, E. B., Pazzaglia, F. J., and Epstein, J. B., 2001, Knickpoint propagation in the Black Hills and northern High Plains: A different perspective on the late Cenozoic exhumation of the Rocky Mountains: Geology, v. 29, no. 6, p. 547-550.

Appendix:

A1: The carbonate cap

The three suggested categories of the carbonate cape overlying the Santa Isabel escarpment are: 1) it is pedogenic, 2) it is an amalgamated high plains calice, or 3) it is a vadose carbonate. The characteristic features of a pedogenic carbonate in thin section include irregularly formed microcrystalline laminae developed on the weathering surface (Scholle et al., 2003).This type of carbonate usually forms in sub humid to arid environments. Maganese blackened pebbles and hairline fractures are also common features (Scholle et al., 2003). A high plains caliche would typically carry irregularly shaped grains called soils pisoids and small amounts of pedogenic carbonate which has enveloped large inclusions of detrital terrigenous silt and sand. Circumgranular cracking is also common, (Scholle et al., 2003). While these type of pisoids grow with a preferential orientation downward, this will not necessarily be visible in the sample as they are most often subsequently rotated into varying positions over extended (100,000-1mya) periods of time. Vadose carbonates form due to a fluctuating water table, which is reflected by gravitational cements that form on the bottom of grains in the same manner and location that water would. Another common characteristic of vadose carbonates is that the tops of the grains are often eroded (Scholle et al., 2003). These listed characteristics are the basic defining features which the thin sections were examined for. The following selection of photographs are representative of some of the common textures, especially those which correlate with the characteristics described above.

Figure A1.1 A carbonate nodule in hand sample, with visible laminations and central matrix material.
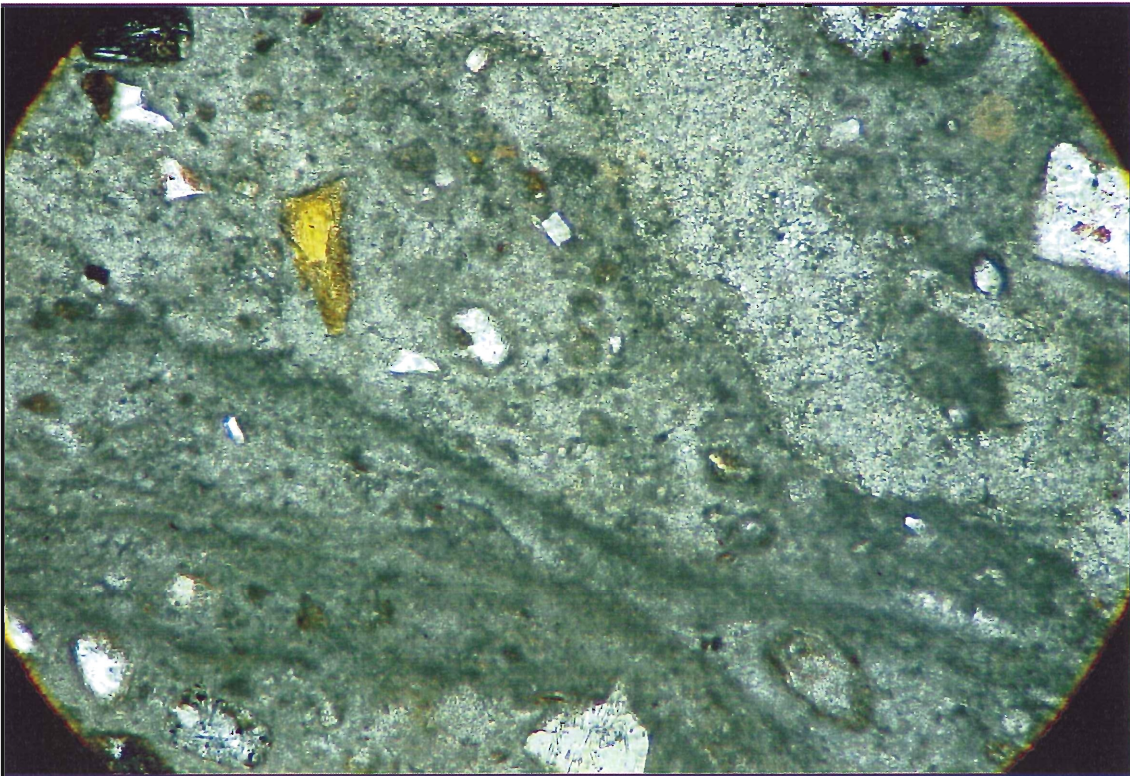
Figure A1.2 The sample in thin sections, showing laminations and various detrital grains.
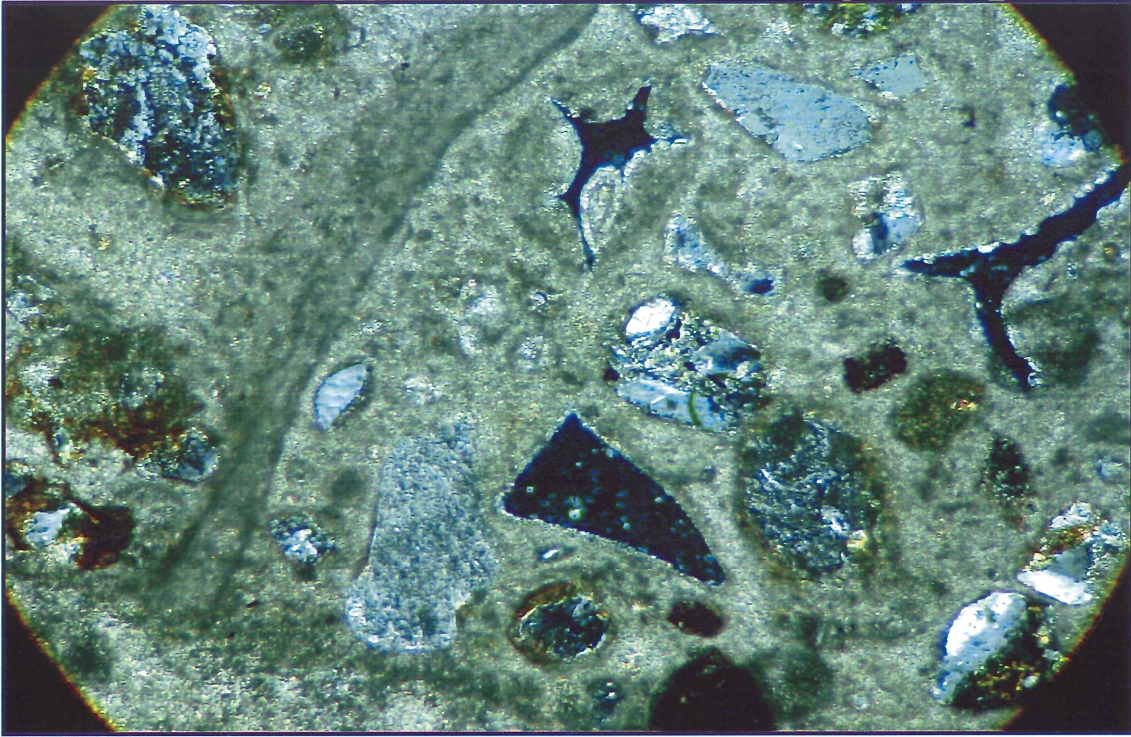
Figure A1.3 Thin section in cross nicols, showing the opaque infilled glass shard in the upper central and upper right corners, as well as visible laminations and reaction rims.

Figure A1.4 The boundary between a large amalgamated central material zone, containing plagioclase and quartz as a fine grained matrix and interstitial grains.
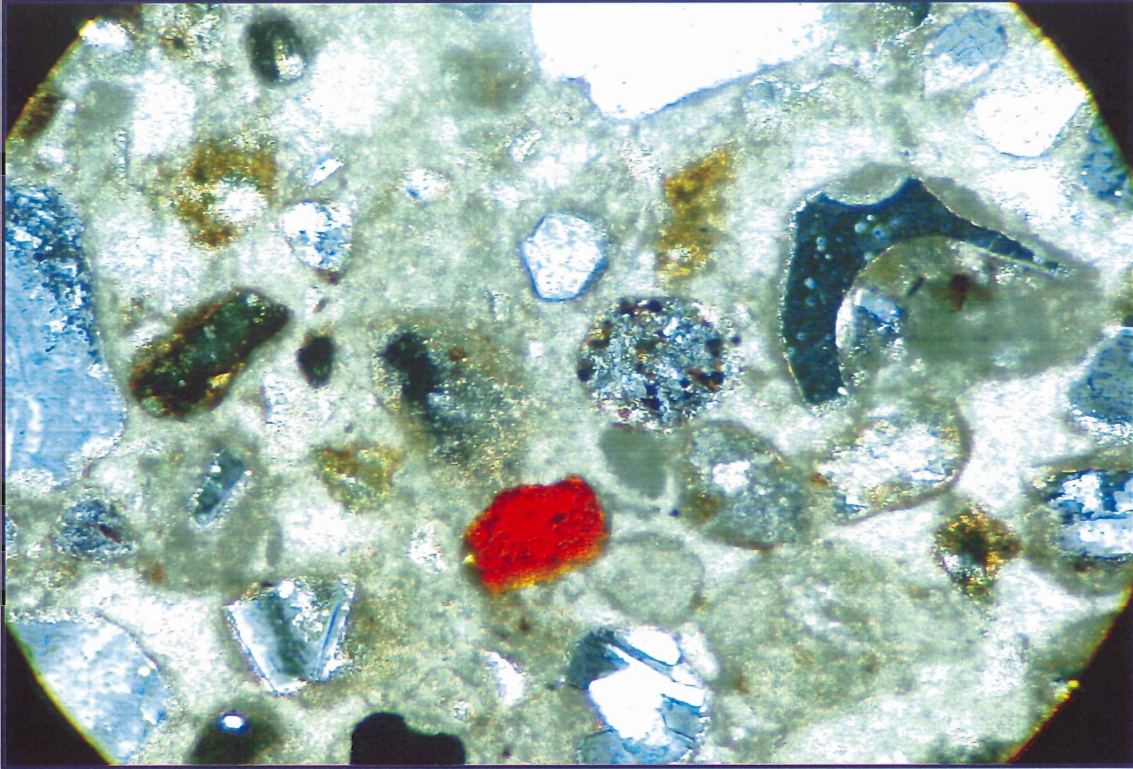
Figure A1.5. (cross nicols) A different location of central matrix material, showing scattered grains including plagioclase, quartz, hematite, and a large infilled glass shard within a cryptocrystalline (presumed calcic) matrix.

Basic Petrography:

Overall, this finely laminated carbonate holds a large contingent of grains in the matrix material which are primarily igneous in nature (being plagioclase, feldspar, quartz, olivine and glass shards). Various other grains were observed in lesser amounts, including hematite, opaques, and possible organics. These were found intermingled with interesting features observed, including the presence of a reaction rim of sorts on many of the grains, the infilling of unusual shaped voids left by the dissolution of glass shards with calcic material, and the dissolution of some of the coarse igneous grains in the matrix. The central material is inequigranular, with a cryptocrystalline matrix. The grains range from subheadral to euheadral, while the glass shards form unusual fragmented shapes. The laminated material is very fine grained, and presumably primarily calcic in nature. Though these brief observations do not lend any hard evidence as to the nature of the genesis of the carbonate, at this time it is most closely correlated though visual example with the features of a pedogenic carbonate.